Research Square

Preprints are preliminary reports that have not undergone peer review.
They should not be considered conclusive, used to inform clinical practice,
or referenced by the media as validated information.

# Evolutionary diversity eclipsed by morphological resemblance in the diatom genus Nitzschia Hassall (Bacillariaceae)

**Rafał M. Olszyński**

rafal.olszynski@biol.uni.lodz.pl

University of Łódź

**Carlos E. Wetzel**

Luxembourg Institute of Science and Technology

**David G. Mann**

IRTA-Institute for Food and Agricultural Research and Technology

**Piotr K. Zakrzewski**

Medical University of Lodz

**Łukasz Peszek**

University of Rzeszów

**Julia Sulkowska**

University of Łódź

**Joanna Żelazna-Wieczorek**

University of Łódź

**Ewa Górecka**

University of Szczecin

**Magdalena Gapińska**

University of Łódź

**Rosa Trobajo**

IRTA-Institute for Food and Agricultural Research and Technology

**Article**

**Keywords:** epitypification, Nitzschia eclipsis, valve ultrastructure, multigene phylogeny, DNA metabarcoding, molecular biogeography

**Posted Date:** November 20th, 2026

**DOI:** https://doi.org/10.21203/rs.3.rs-11623458/v1

**License:** This work is licensed under a Creative Commons Attribution 4.0 International License.
Read Full License

**Additional Declarations:** No competing interests reported.

## Abstract

Shared morphological character states may represent synapomorphies, retained ancestral states or homoplasies; resemblance alone cannot distinguish them, especially when historical names lack secure links to diagnostic morphology and molecular lineages. We investigated a Polish post-mining population initially identified as *N.* cf. *archibaldii* using type-based morphology, an SSU–*rbc*L–*psb*C phylogeny and environmental *rbc*L metabarcoding. Re-examination of the *N. archibaldii* holotype and designation of an epitype clarified the application of the name. Differences in terminal raphe fissures and the valve face–mantle junction support recognition of the Bogdałów population as *N. eclipsis* sp. nov. Both cultured strains formed a maximally supported lineage within clade 6B. *N. eclipsis* was sister to a clade with contrasting valve outlines, showing that overall resemblance alone cannot establish close relationships within clade 6B. Without DNA from unequivocally identified *N. archibaldii*, its phylogenetic placement and relationship to *N. eclipsis* remain unresolved. Among 41 environmental *rbc*L datasets, exact short-barcode matches occurred in two Spanish samples and a one-nucleotide variant in samples from the United States, suggesting occurrences beyond Poland but not defining a species range. Species delimitation, phylogenetic placement and geographical distribution therefore require different evidence and may be resolved to different degrees.


## Introduction

Species-level identification is central to reconstructing diatom evolutionary relationships and interpreting their ecological and geographical distributions. Diatom species have long been delimited mainly by frustule morphology, although studies of sexual reproduction have shown that some traditionally recognised species include reproductively isolated groups [1]. Mann [2] subsequently argued that diatom species boundaries had often been drawn too broadly and advocated using evidence from morphology, mating behaviour, genetics and ecology to investigate them. Integrative studies have shown that widespread morphospecies may contain distinct genetic lineages, including the *Sellaphora pupula* (Kützing) Mereschkovsky, 1902, *Gomphonema parvulum* (Kützing) Kützing, 1849 and *Eunotia bilunaris* (Ehrenberg) Schaarschmidt, 1880 complexes [3–5].

The challenge of recognising species with limited morphological evidence is especially apparent in *Nitzschia* Hassall, 1845, one of the largest genera of pennate diatoms. Many of its species are small-celled, delicately silicified, and offer few discrete characters that can be reliably assessed using light microscopy [6, 7]. Traditionally, *Nitzschia* was subdivided into sections, based mainly on valve shape and symmetry, the position of the raphe system, the morphology of the fibulae and the visibility of the striae [8]. Molecular analyses, however, have shown that *Nitzschia* is non-monophyletic, with other genera (*Simonsenia* Lange-Bertalot, 1979, *Denticula* Kützing, 1844, *Cylindrotheca* Rabenhorst, 1859 and others) nested within it and that most of its traditional sections do not represent natural evolutionary lineages. In particular, the section *Lanceolatae*, traditionally comprising species with narrow linear to lanceolate valves and strongly eccentric raphe systems, is polyphyletic [6, 7]. However, some species traditionally assigned to the *Lanceolatae* form well-supported molecular lineages, notably clade 6B sensu Mann et al.

[7] which includes *N. palea* (Kützing) W. Smith, 1856, *N. capitellata* Hustedt, 1930, *N. lembiformis* F. Meister *ex* Clavero, 2009, *N. pusilla* Grunow, 1862 and *N. excavata* Olszyński, D.G. Mann & Trobajo, 2026. Within clade 6B are a number of delicate, finely striated taxa that have always been taxonomically difficult and cannot be reliably distinguished from one another using light microscopy (LM) alone. Electron microscopy shows some structural differences among clade 6B species (such as differences in the structure of the raphe canal walls and girdle bands, specifically whether they bear one longitudinal row of poroids or two). However, these features can vary even between closely related strains (e.g. within the *N. palea* complex: Mann et al. [7], p. 11) and have not been identified as defining traits of specific subgroups within clade 6B. Furthermore, the lack of distinctive characteristics visible in LM makes it very difficult to plan sampling for morphological and molecular analysis, and it is unclear whether taxon coverage is poor, adequate or good. Overall, therefore, it often remains unclear whether the morphological similarities between the finely striated, *Lanceolatae*-like taxa of clade 6B reflect close evolutionary relationships, homoplasies, or the retention of plesiomorphic character states.

*Nitzschia excavata* illustrates this problem: morphologically it resembles *N. palea* to such an extent that it must often have been misidentified as *N. palea* in floristic enumerations and routine LM-based biomonitoring (there is a difference in stria density between the two, but this can be determined only by electron microscopy), but a three-marker phylogeny has confirmed it as a distinct lineage [9]. Because of possible confusion with *N. palea* in LM, the distributions of the two species can be securely determined only by using DNA barcodes. Searches of environmental sequence data reveal that the *N. excavata* lineage, or closely related variants, occurs in several geographically distant freshwater habitats [9], but it seems to have a much more restricted ecological range than *N. palea*. *Nitzschia excavata* was isolated from the Bogdałów reservoir in west-central Poland, formed in a former lignite open-pit mine, and a further new *Nitzschia* species has also been described from the reservoir, namely *Nitzschia nandorii* Olszyński, Zakrzewski & Żelazna-Wieczorek, 2024. Further surveys have revealed additional previously undocumented diatom diversity in an otherwise well-studied region of Poland [9–11]. This included the small, linear-lanceolate *Nitzschia* analysed in the present paper, which was provisionally identified as *N.* cf. *archibaldii*, although its morphology did not permit confident assignment to any known species. The provisional identification also made it necessary to reassess the morphological application of the name *N. archibaldii* Lange-Bertalot, 1980.

Accordingly, the identity and evolutionary relationships of the *archibaldii*-like population from Bogdałów were assessed using an integrative morphological and molecular approach. A multigene phylogeny based on nuclear SSU rDNA and the plastid markers *rbc*L and *psb*C was combined with comparative examination of *N. archibaldii* material and environmental *rbc*L metabarcoding to delimit the Bogdałów lineage, assess its potential distribution, formally describe *Nitzschia eclipsis* sp. nov., and clarify the morphological application of the name *N. archibaldii* through epitypification.

## Materials and methods

# 1.1 Study sites

The new species studied here was obtained from the Bogdałów reservoir, located near the village of Bogdałów in the Greater Poland Voivodeship, west-central Poland, northeast of Turek (approximately 52°02'53.9" N, 18°35'49.6" E). The reservoir occupies the remaining depression of the former Bogdałów lignite open pit within the Konin–Turek mining district and was created during reclamation of the excavation in 1993–1994 [9, 10, 12, 13]. The resulting waterbody covers approximately 10 ha and has a storage capacity of approximately 0.6 million m³. Its hydrological conditions are influenced by an inflowing small watercourse and drainage waters from the surrounding mining area. The reservoir is now surrounded mainly by secondary woodland dominated by pine and birch [12–15].

# 1.2 Sampling and cultures

Sampling and single-cell isolation followed the procedures described by Olszyński et al. [9, 10]. Strain D.LDZ5 was isolated from a sand sample from the bottom of the Bogdałów reservoir in October 2022 (D.BOZS.191022) during the sampling campaign described by Olszyński et al. [10]. Another sample, D.BOZM.221024, was collected from the reservoir on 22 October 2024 and included because the taxon described here was also observed in this material. Strain D.LDZ23 was isolated from sample D.BOZL.191125, collected from submerged stones on 19 November 2025. During the 2025 sampling, separate subsamples were collected using sterile, single-use tools. Material intended for the preparation of permanent diatom slides was immediately preserved by adding ethanol to a final concentration of 70% (v/v), following Baričević et al. [16] and EN 13946:2025 [17], whereas material intended for single-cell isolation and culture establishment was kept unfixed.

Water temperature and electrical conductivity were measured in situ using a CC-411 conductivity meter, pH using a CP-401 pH meter, and dissolved oxygen using a CO-401 oxygen meter (ELMETRON, Poland). An additional water sample was collected on 19 November 2025 in sterile 50-mL polypropylene centrifuge tubes. Concentrations of orthophosphate ($PO_4^{3-}$), ammonium ($NH_4^+$), calcium ($Ca^{2+}$), magnesium ($Mg^{2+}$), potassium ($K^+$), nitrite ($NO_2^-$), nitrate ($NO_3^-$) and chloride ($Cl^-$) were determined spectrophotometrically using a Spectroquant® Pharo 100 spectrophotometer and the corresponding Spectroquant® test kits (Merck KGaA, Darmstadt, Germany), following the manufacturer's instructions. Three separate aliquots of the same water sample were processed independently, with reagents added separately to each aliquot. Results are reported as mean ± SD (n = 3), and concentrations below the analytical range of a test are reported as below the corresponding detection or quantification limit.

Single diatom cells were isolated from the unfixed material, and monoclonal cultures were established in sterile Bacillariophycean Medium (Sammlung von Algenkulturen Göttingen Medium Recipe Culture Collection of Algae) and maintained under the conditions described by Olszyński et al. [9, 10]. Morphological characterisation by LM included environmental samples D.BOZM.221024 and D.BOZL.191125 and strains D.LDZ5 and D.LDZ23. SEM observations were based on all environmental samples and both strains, whereas TEM examination was restricted to strain D.LDZ23.

# 1.3 Comparisons with *Nitzschia archibaldii*

Initial examination of samples and strains from Bogdałów reservoir led to a provisional identification of the material as *Nitzschia* cf. *archibaldii* [18]. However, the identification remained uncertain because of the heterogeneity of the valve outline in published descriptions (in particular, the difference between Fig. 18 and Figs. 14–17 in Lange-Bertalot [18], and the range of shapes and sizes given in two key identification texts, Krammer and Lange-Bertalot [19]; Lange-Bertalot et al. [20]) and the apparent lack of any characters that could confirm the identification of the finely structured forms found at Bogdałów. Therefore, the holotype slide of *Nitzschia archibaldii*, prepared by Professor Horst Lange-Bertalot, was examined and photographed using LM. The slide is labelled “Bad Homburg, Braumannswiesen, 1975” and “*Nitzschia archibaldii* Lange-B., Holotyp” and bears the handwritten reference “Zu 2/30” (Fig. 1A). To locate unmounted material from the type gathering suitable for ultrastructural examination, we contacted Professor Lange-Bertalot himself, the Botanic Garden and Botanical Museum Berlin, and the Senckenberg Research Institute and Natural History Museum Frankfurt. Dr Andrew-Charles Podzorski of the Senckenberg diatom collection also searched the holdings of the H. Lange-Bertalot collection. Despite this exhaustive search, no corresponding unmounted material was found. The available type material therefore appears to be restricted to a single permanent slide, limiting direct comparison with the type material to LM examination and five transmission electron micrographs published by Lange-Bertalot ([18], Figs. 115–121).

Because of the very restricted possibilities to examine original and authenticated material of *N. archibaldii*, and in order to determine how other workers have interpreted the species, we also examined four archived environmental samples from the French diatom monitoring network, all of which contained an abundance of valves that had previously been identified as *Nitzschia archibaldii*:

- Sample 1189 HA: River Jouques (Var department); collected May 18, 2012. Leg. Christine Chambert. Identified as *N. archibaldii* by Luc Ector
- Sample 1721 HA: Hérault River at Valleraugue (Gard department); collected July 5, 2013. Leg. Rémy Marcel. Identified as *N. archibaldii* by Luc Ector
- Sample 2123 HA: Étang du Vignoble, labelled "Racines" (Valenciennes, Nord department, Hauts-de-France region); collected October 7, 2015. Leg. Nathalie Zydek. Identified as *Nitzschia* cf. *archibaldii* by Luc Ector
- Sample 4794 HA: L’Automne River at Bémont (Oise department, Hauts-de-France region); collected October 4, 2024. Leg. David Fouré. Identified as *N. archibaldii* by Carlos E. Wetzel

# 1.4 Microscopy

Microscopic analyses included environmental samples D.BOZS.191022, D.BOZM.221024 and D.BOZL.191125 and monoclonal strains D.LDZ5 and D.LDZ23. The chloroplast structure of living cultured cells of strain D.LDZ5 was examined using a Nikon Eclipse E400 light microscope (Nikon, Japan) equipped with a 100×/1.40 Plan APO DIC H oil-immersion objective and an OPTA-TECH HDMI-series camera with a resolution of 3840 × 2040 pixels and a 1/2.7" Sony sensor. Diatom frustules from

environmental and cultured materials were cleaned following the oxidation procedure of Żelazna-Wieczorek [21] and detailed by Olszyński et al. [9, 10]. The cleaned material was mounted on permanent slides in Naphrax resin (Brunel Microscopes Ltd., UK). Cleaned valves from strain D.LDZ23 were examined and measured using the Nikon Eclipse E400 system described above. Photomicrographs of strain D.LDZ5 were obtained using a Nikon Eclipse 50i microscope under 1000× magnification, equipped with a 100×/1.25 plan oil-immersion objective and an OPTA-TECH digital camera. Environmental specimens were examined and photographed using a Nikon Eclipse 90i (Nikon, Japan) photomicroscope with a Plan-Apochromat 100× objective (nominal N.A. 1.4); with this objective, the digital camera allowed resolution better than 30 pixels per micrometre. Microscopic observations of *Nitzschia archibaldii* type material were performed using a ZEISS Axioplan microscope equipped with an AxioCam MRc camera and a 100× oil-immersion objective. Images were acquired and analysed using ZEN software at the Botanic Garden and Botanical Museum Berlin, Freie Universität Berlin, Germany. LM morphometric measurements of the specimens from the 4794 HA sample were based on the sample and included valve length, valve width and fibula density expressed as the number of fibulae per 10 µm. Morphometric measurements were carried out at ×1000 magnification using an oil immersion objective on a Leica DMR light microscope (Leica Microsystems, Wetzlar, Germany). Images were captured with a Leica DC500 digital camera and processed using Leica Application Suite (LAS) software at the Luxembourg Institute of Science and Technology (LIST), Luxembourg. At the University of Rzeszów in Poland, SEM observations included cleaned material from strain D.LDZ5 and cleaned and uncleaned material from samples D.BOZS.191022 and D.BOZM.221024, examined as described by Olszyński et al. [9]. SEM examination at the Luxembourg Institute of Science and Technology (LIST) included sample D.BOZL.191125, strain D.LDZ23 and the French samples. Samples were examined using an ultra-high-resolution analytical field emission microscope (FE-SEM Hitachi SU- 70, Hitachi High-Technologies Corporation, Tokyo, Japan) at 5 kV and a 10 mm working distance, using the lower secondary electron (SE-L) detector. Parts of the oxidised suspensions were filtered with additional deionised water through a 3 µm Isopore™ polycarbonate membrane filter (Merck Millipore), pieces of which were affixed to aluminium stubs after air-drying. Filters were coated with a 12 nm platinum layer using a Leica EM ACE600 sputter coater (Leica Microsystems GmbH, Germany). For additional SEM morphometry, cleaned material from strain D.LDZ23 was air-dried onto aluminium stubs and sputter-coated with a 20-nm layer of gold. The valves were examined and measured using a Phenom Pro X scanning electron microscope operated at 10 kV at the Department of Invertebrate Zoology & Hydrobiology, Faculty of Biology and Environmental Protection, University of Lodz, Poland. Transmission electron microscopy (TEM) studies were conducted in the Laboratory of Microscopic Imaging and Specialized Biological Techniques, Faculty of Biology and Environmental Protection, University of Lodz, Poland. For TEM analysis, 10 µl of isolated diatom frustules were placed on 200 mesh copper grids with a formvar/carbon surface (EM Resolutions, Keele, Staffordshire, England) and dried at room temperature. The investigation was conducted using JEM-1010 (JEOL Ltd, Tokyo, Japan), operating at an accelerating voltage of 100 kV. Developed TEM imaging films (EM-Films EMS, MACO, Hans O. Mahn GmbH & CO. KG, Stapelfeld, Germany) were scanned using Perfection V700 PHOTO scanner (Seiko Epson Corp., Suwa, Japan).

Figure plates were prepared using Corel PHOTO-PAINT 2020 (version 22.0.0.412; Corel Corporation, Ottawa, Canada).

## 1.5 DNA isolation, amplification, and sequencing

Genomic DNA was isolated from monoclonal cultures of strains D.LDZ5 and D.LDZ23 using the Chelex® 100 protocol (Bio-Rad, USA), following Dąbek et al. [22] and the procedures described previously [9, 10]. Primer sequences and amplification conditions are presented in Supplementary Table S1 online [23–26]. PCRs were performed with Invitrogen™ Platinum™ II Hot-Start Green PCR Master Mix (2X) (Thermo Fisher Scientific, Waltham, MA) in 25 µL reactions according to the manufacturer's protocol. All amplifications were performed in triplicate to obtain products suitable for sequencing. Amplification products were checked on 1% agarose gels. PCR product purification and Sanger sequencing were performed by SEQme s.r.o. (Czech Republic). Forward and reverse reads were assembled and manually inspected using Geneious Prime® 2023.2.1 (Biomatters Inc., USA).

## 1.6 Sequence alignment and phylogenetic analyses

Taxon sampling was based on Mann et al. [7] and supplemented with relevant sequences subsequently deposited in GenBank (NCBI) and those generated in this study. Sequences from diatom endosymbionts of dinoflagellates were retained because they represent bacillariacean genetic material rather than sequences of the dinoflagellate hosts [27–29]. Phylogenetic analyses were performed separately for SSU rDNA, *rbc*L and *psb*C, and for a concatenated SSU–*rbc*L–*psb*C matrix.

Single-marker analyses assessed congruence among markers and the placement of the studied strains, particularly because SSU rDNA was unavailable for D.LDZ5. *Eunotia bilunaris* (Ehrenberg) Schaarschmidt, 1880 strain UTEX FD412 served as the outgroup in both the single-marker and concatenated analyses. For taxa with incomplete marker sampling, the corresponding regions of the concatenated matrix were treated as missing data. Voucher information and GenBank accession numbers are provided in Supplementary Data S2 online.

Each marker was aligned using the MAFFT v. 7 web server with the Auto strategy [30] following Olszyński et al. [9, 10], and the resulting alignments were manually inspected and corrected where necessary. For each single-marker dataset, the best-fitting nucleotide substitution model was selected using ModelFinder as implemented in IQ-TREE, according to the Akaike Information Criterion (AIC) [31].

The concatenated matrix was divided into seven initial partitions: three codon positions for *rbc*L (reading frame + 1), three for *psb*C (reading frame + 3) and one unpartitioned SSU rDNA subset. Partition merging and model selection in IQ-TREE under AIC retained all seven partitions [31, 32] GTR + F+I+G4 was selected for all three *rbc*L codon positions and for the first and third *psb*C codon positions, whereas TIM3 + F + I+G4 was selected for the second *psb*C codon position and SSU rDNA.

The single-marker alignments comprised 202 SSU rDNA sequences and 1470 positions, 327 *rbc*L sequences and 1357 positions, and 124 *psb*C sequences and 1026 positions. The concatenated matrix

contained 224 taxa and 3603 positions: *rbc*L positions 1–1107, *psb*C positions 1108–2133 and SSU rDNA positions 2134–3603.

Maximum-likelihood analyses were performed in IQ-TREE version 3.0.1 [33], with branch support assessed using 10,000 ultrafast bootstrap replicates (UFBoot) [34], 10,000 SH-aLRT replicates [35] and the approximate Bayes test [36]. The tree search was terminated after 1,000 unsuccessful iterations. The concatenated and separate *rbc*L phylogenies are presented, whereas the *psb*C and SSU rDNA analyses were used to assess congruence among markers.

Bayesian inference of the concatenated matrix was performed in MrBayes version 3.2.7a [37] using the same seven partitions as in the ML analysis. Because TIM3 is unavailable in MrBayes, GTR + I + Γ4 was applied to all partitions, with model parameters estimated independently and relative rates allowed to vary among partitions. Two independent runs, each comprising six Metropolis-coupled Markov chains, were conducted for up to 50 million generations, with the heating parameter set to 0.06 and six swap attempts per generation. Trees were sampled every 100 generations. The analysis terminated automatically at 11,886,000 generations after the average standard deviation of split frequencies (ASDSF) fell below 0.01. Convergence was additionally assessed using potential scale reduction factors and effective sample sizes for model parameters. After discarding 25% of the samples from each run as burn-in, posterior probabilities were calculated using a 50% majority-rule consensus. Computations were performed using the MPI-enabled version of MrBayes with 12 parallel processes on the Tryton Plus supercomputer at CI TASK, provided through the PLGrid infrastructure.

The resulting phylogenetic trees were visualised and annotated using Interactive Tree Of Life [38]. Final alignments, partition and analysis files, and consensus trees are provided in Supplementary Data S3 online.

# 1.7 Metabarcoding distribution analysis

The geographical distribution of the new species was investigated by probing available *rbc*L metabarcoding datasets with the *rbc*L sequence for one of the isolates, D.LDZ5 (GenBank: PZ881546). The method was described by Olszyński et al. [9] and included downloading the fastq files of available metabarcoding datasets (principally from the Short Read Archive of NCBI); processing them through a DADA2 pipeline [39], with the error modelling adjusted as necessary for those datasets with binned phred scores; consolidating the Amplicon Sequence Variants (ASV) into a few combined datasets; and searching the fasta files derived from the combined sets by local BLAST [40] using the D.LDZ5 sequence as the query. The combined metabarcoding datasets included 41 metabarcoding datasets (over 11,000 samples) from all continents except Australia but were biased towards Europe and N. America; they are listed in Supplementary Data S4 online.

Again, as done by Olszyński et al. [9], NCBI metagenomic datasets for matches to D.LDZ5 sequences were explored using the NCBI PebbleScout tool (Shiryev & Agarwala, 2024).

## Results

# 1.8 Morphological reassessment and epitypification of *Nitzschia archibaldii*

Morphological reassessment confirmed the identification of samples 1189 HA, 1721 HA and 4794 HA as *Nitzschia archibaldii*. However, specimens from sample 2123 HA did not conform to the type concept of the species due to the presence of a wider interspace between the two central fibulae and were therefore excluded from further analysis; representative micrographs are provided in Supplementary Figure S5 online. LM morphometry and selection of the epitype were based on sample 4794 HA (Fig. 2), whereas comparative SEM observations were conducted on samples 1189 HA, 1721 HA and 4794 HA. All four archived samples are stored at the Luxembourg Institute of Science and Technology (LIST). A virtual slide (LM) for sample 4794 HA can be found in Heudre and Wetzel [42].

*Nitzschia archibaldii* Lange-Bertalot, Bacillaria 3: 44, pl. 1, Figs. 14–18; pl. 7, Figs. 115–121. 1980.

**Holotype** (supported by the epitype designated below and explicitly cited here): GERMANY. Hesse: Bad Homburg, Braumannswiesen, in an unpolluted stream, growing on *Phormidium* crusts, 1975, permanent slide Zu 2/30, B 40 0051142, PhycoBank 107558, Repository: B – ZE Botanischer Garten und Botanisches Museum, Freie Universität Berlin (Fig. 1A).

**Epitype** (designated here): FRANCE. Hauts-de-France region, Oise department, L'Automne River at Bémont, epilithon, 4 October 2024, leg. David Fouré, sample 4794 HA; the valve illustrated in Fig. 2P, on permanent slide SZCZ 30013, electronic scan of slide available under https://doi.org/10.5281/zenodo.22896583, deposited in the Szczecin Diatomological Collection, University of Szczecin, Poland

**PhycoBank registration**: (epitype): http://phycobank.org/107820

**Rationale for epitypification**. The holotype preparation permits examination of valve outline and fibula arrangement in LM but does not allow the diagnostically important ultrastructural characters to be reassessed. Even the stria density remains impossible to demonstrate in the holotype because it is at or beyond the resolution of the light microscope, though Lange-Bertalot showed from TEM that it is over 48 in 10 µm. Because the LM features overlap with those of Bogdałów *N.* cf. *archibaldii* population and other finely striated *Nitzschia* taxa, the holotype alone does not permit unambiguous characterisation of the species and therefore application of the name using the characters required for species delimitation. No unmounted material from the original gathering could be located despite searches of the relevant collections. Following Article 8.2 of the ICN [43], sample 4794 HA was selected for epitypification because its valves agree with the holotype in LM, while material from the same gathering documents by SEM the short, weakly hooked terminal raphe fissures and the absence of the strongly recurved fissures and conspicuous apical siliceous flap characteristic of *N.* cf. *archibaldii* from Bogdałów3.2. The epitype

therefore links the LM morphology of the holotype (Fig. 1B–P) and the ultrastructural information provided in the protologue to permanently preserved material available for renewed examination.

**Epitype population**, sample 4794 HA (Figs. 2, 3D, I). In LM, valves are 13.8–21.8 µm long and 2.6–3.5 µm wide (n = 20). Striae are not resolvable. Fibulae are distinct and irregularly spaced, numbering 14–17 in 10 µm (n = 20) (Fig. 2). SEM observations show a flat valve face, with the virgae not visibly raised above the adjacent areolate areas (Fig. 3D). On the distal side, the valve face–mantle junction is poorly delimited, with the striae continuing smoothly onto the mantle (Fig. 3D). The external raphe slit is continuous and lacks proximal endings (Fig. 3D). The wall of the raphe canal bears a single longitudinal row of areolae (Fig. 3I), some of which are subdivided by additional vimines towards the centre of the valve (Fig. 3D). The second valve in Fig. 3D is shown in internal view and has narrow, unornamented, irregularly spaced fibulae without a distinctly wider central interspace. The visible striae are uniseriate and composed of elliptical areolae (Fig. 3I). The terminal raphe fissures are short and weakly hooked, with their curved portions confined to the valve apices rather than extending appreciably onto the valve face or mantle (Fig. 3I).

**Additional French populations of N. archibaldii examined by SEM** (samples 1189 HA and 1721 HA; Figs. 3A–C, E–H). Together, these specimens confirm the principal features observed in the epitype population: a flat valve face with virgae not visibly raised above the adjacent areolate areas (Figs. 3A–C), a poorly delimited distal valve face–mantle junction (Fig. 3A), and uniseriate striae composed of elliptical areolae of relatively uniform shape and size (Figs. 3A, B, F–H). They also confirm a continuous external raphe slit without proximal endings (Figs. 3B, C, F), short, weakly hooked terminal fissures confined to the valve apices (Figs. 3G, H), and a predominantly single longitudinal row of poroids on the external wall of the raphe canal (Figs. 3C, G, H).

Beyond confirming these shared characters, the additional material provided further ultrastructural detail on the raphe canal wall, girdle bands and fibulae. Locally, two rows of poroids are visible on the raphe canal wall (Figs. 3G, H), as in the specimens illustrated in TEM by Lange-Bertalot ([18], Fig. 121). Some of these poroids are wider than the areolae on the valve face, probably owing to local reduction or loss of the intervening vimines (Figs. 3G, H). The valvocopulae bear two longitudinal rows of well-developed poroids (Figs. 3F–H). At least one advalvar girdle band terminates laterally on the frustule, with an obliquely tapered end forming a wedge-shaped junction with an adjacent band (Figs. 3A, F). Internal views likewise confirm the narrow, unornamented and irregularly spaced fibulae, without a distinctly wider central interspace (Figs. 3C, E), and additionally show that individual fibulae are usually connected to two virgae (Fig. 3E).

# 1.9 Taxonomic treatment

**Nitzschia eclipsis Olszyński and D.G. Mann, sp. nov.** Figures 4–7

**Diagnosis**. In LM, *Nitzschia eclipsis* is very similar to *N. archibaldii* but differs in having gradually tapering, narrowly rounded, non-capitate apices and more regularly spaced fibulae. It is further distinguished

ultrastructurally from the French populations assigned to *N. archibaldii*, including the *N. archibaldii* epitype, by its strongly recurved terminal raphe fissures associated with a conspicuous siliceous apical flap, a distinctly delimited junction between the valve face and distal mantle, and a valvocopula bearing a single longitudinal row of well-developed poroids rather than two rows.

**Holotype**. The specimen indicated in Fig. 4M on permanent slide D.BOZL.191125, prepared from the type material collected on 19 November 2025 and deposited in the Algae Collection of the Department of Algology and Mycology, University of Lodz, Poland.

**Isotype**. Permanent slide SZCZ 29882, prepared from the same type material and deposited in the Szczecin Diatomological Collection, University of Szczecin, Poland.

**Type locality**. POLAND, Greater Poland Voivodeship, Bogdałów post-mining reservoir, 52°02'53.938" N, 18°35'49.646" E; epilithic material collected from stones on 19 November 2025.

**Etymology**. The specific epithet *eclipsis*, derived from a Latinised Greek noun meaning “eclipse”, refers to the total solar eclipse of 12 August 2026, visible from La Ràpita, Catalonia (where part of the taxonomic work leading to the description of the species was carried out), which four of us (RMO, PKZ, DGM and RT) had the privilege to enjoy together. The name also alludes to how the species’ distinct evolutionary identity was eclipsed by its morphological resemblance to *N. archibaldii* and revealed through integrative taxonomic and phylogenetic analyses.

# Description

The following morphological observations are based on both environmental material (including the type material) and cultured strains. *Nitzschia eclipsis* has two plastids that are elongated and curved in cross-section, running along the valve and onto the girdle to create a semi-tubular formation. (Fig. 4A–J). Small granules, presumably volutin, are produced at the apex of each chloroplast and are easily seen under light microscopy. (i.e. Figure 4F, J). The valves are narrowly linear-lanceolate, with slightly convex margins gradually tapering to narrowly rounded apices (Fig. 4K–E'). Based on LM and SEM measurements, the valves are 22.0–26.4 µm long and 2.0–3.0 µm wide (n = 34) with 44–47 striae in 10 µm (n = 17), which are not resolvable in LM. The fibulae are distinct but small in LM, fairly evenly spaced, and number 12–21 in 10 µm (n = 29).

The valve face is essentially flat and externally the virgae appear slightly raised relative to the adjacent striae (Figs. 5A, B, E, 6D, E), which are uniseriate and contain simple poroid areolae occluded by hymenes close to the external openings (Figs. 5E, 6A–C). The areolae are predominantly subquadrate rather than circular (Figs. 5E, 6C). Along the raphe canal wall, two longitudinal rows of poroids are generally present on both the valve-face side (Fig. 6E, F) and the mantle side of the raphe (Fig. 6D). Locally, reduction of the intervening vimines results in fusion of neighbouring poroids and the formation of transapically elongate openings (Fig. 6C, E). The junction between the valve face and the distal mantle is distinct (Figs. 5B, 6E), with a clear break in the striae, while the distal mantle bears one longitudinal row of

elongate poroids (Fig. 6E). The proximal mantle bears predominantly elongate poroids and is clearly differentiated from the raphe canal wall (Fig. 6D).

The raphe is strongly eccentric and lacks central raphe endings (Fig. 6B). At the apices, the terminal raphe fissures are strongly hooked and may be deflected towards either the distal or proximal side of the valve through nearly 180° (Figs. 5F, 6A, C). In both orientations, the terminal fissure is associated with a conspicuous apical flap (Figs. 5F, 6A, C). This apical structure is particularly well developed where the terminal fissure is strongly recurved. On the side of the raphe canal adjacent to the proximal mantle, its wall is perforated by poroids that are locally elongate (Figs. 5F, G, 6D).

Internally, the valve face is flat and lacks additional siliceous structures (Fig. 5C, D). The raphe canal is separated from the valve face by short, narrow and regularly spaced fibulae, without a wider central interspace (Fig. 5D). The fibulae are smooth and lack ornamentation. Each is usually connected transapically to two virgae (Fig. 5G) and longitudinally by a slender ridge to the adjacent fibula. Through the portulae (i.e. between the fibulae) the transapical striae can be seen continuing onto the wall of the raphe canal (Fig. 5D, G). At each pole, the distal raphe end terminates internally in a well-developed helictoglossa (Fig. 5G). No central nodule or internal central raphe endings are present.

The girdle is incompletely known but it is clear that (1) the valvocopula is ornamented by a single longitudinal row of relatively large, well-developed poroids (Figs. 5E, 6A, C, F) and (2) at least one advalvar girdle band has a lateral, obliquely tapered end (rather than ending at the valve pole), forming a wedge-shaped junction with an adjacent band (Fig. 5C). In Fig. 6A, the poroids on a girdle band become indistinct towards one end of the valve, possibly reflecting the lateral band termination, although the junction itself is not clearly resolved.

TEM observations confirm the regular arrangement of the uniseriate transapical striae and the short, regularly spaced fibulae, without a visibly wider central interspace (Fig. 7A, B). The terminal raphe fissures are clearly visible at the valve apices (Fig. 7A, C, D). They are strongly recurved and may turn through nearly 180° around a conspicuous apical siliceous flap (Fig. 7D, curved arrow in Fig. 7F). The apical siliceous flap is present at the valve apex (Fig. 7E, F).

**Reference strains and DNA sequences**

Two monoclonal strains were included in the molecular analyses. Strain D.LDZ5 was isolated from environmental sample D.BOZS.191022 and is treated as an additional reference strain. Strain D.LDZ23 was isolated from the type material D.BOZL.191125 and is retained as the reference strain established from the type material.

The *rbc*L and *psb*C sequences were obtained for both strains, whereas the SSU rDNA sequence was obtained only for D.LDZ23. The sequences were deposited in GenBank under the following accession numbers: D.LDZ5—*rbc*L: PZ881546, and *psb*C: PZ881544, D.LDZ23—SSU rDNA: PZ871626, *rbc*L: PZ881547, and *psb*C: PZ881545.

**PhycoBank registration**: http://phycobank.org/107763

# 1.10 Phylogenetic placement of *Nitzschia eclipsis*

Phylogenetic analysis of the concatenated SSU–*rbc*L–*psb*C dataset recovered two strains D.LDZ5 and D.LDZ23, of *Nitzschia eclipsis* as a distinct, maximally supported lineage (UFBoot = 100; PP = 1). The lineage was placed within clade 6B of the *Bacillariaceae* sensu Mann et al. [7], in a group containing several finely striated, *Lanceolatae*-like *Nitzschia* taxa (Fig. 8).

The lineage formed by D.LDZ5 and D.LDZ23 was recovered as sister to a larger, maximum supported clade (UFBoot = 100; PP = 1) comprising two principal lineages (Fig. 8). The first includes *N.* cf. *ardua* L44, *Nitzschia* sp. SZCZCH1090 and *N. excavata* and received maximum support (UFBoot = 100; PP = 1). Within this lineage, *N. excavata* was most closely related to *Nitzschia* sp. SZCZCH1090 (UFBoot = 100; PP = 1), whereas *N.* cf. *ardua* L44 was sister to this pair (UFBoot = 92; PP = 1). The second lineage comprised *N. pusilla* strains TA420 and TA-45 together with *N. lembiformis* R2 and was strongly supported (UFBoot = 95; PP = 0.96).

More broadly, *Nitzschia eclipsis* was placed within clade 6B, one of the phylogenetic lineages containing taxa traditionally assigned to the morphologically defined *Lanceolatae*. Clade 6B comprised predominantly morphologically similar, narrow and finely striated taxa with linear to lanceolate valve outlines. Within this clade, strains D.LDZ5 and D.LDZ23 formed a distinct and strongly supported lineage.

In the single-gene phylogeny of *Nitzschia* clade 6B based on long *rbcL* sequences (Supplementary Figure S6 online), the two strains of *N. eclipsis* formed a distinct clade sister to a lineage comprising *N. excavata*, *Nitzschia* sp. SZCZCH1090, *N.* cf. *ardua* L44 and *N. communis* TCC853. However, this relationship received only low support (UFBoot = 64). This entire clade was, in turn, sister to a lineage comprising two strains of *N. pusilla* and *N. lembiformis* (UFBoot = 99). This topology differed slightly from that recovered in the concatenated analysis, in which *N. eclipsis* was sister to the entire clade comprising all of the above-mentioned strains (Supplementary Figure S6 online).

# 1.11 Environmental conditions at the type locality of *N. eclipsis*

At the time of sampling on 19 November 2025, water temperature was 7.7°C, pH 8.11, dissolved oxygen concentration 8.09 mg $L^{-1}$ and electrical conductivity 602 µS $cm^{-1}$. Calcium, magnesium, nitrate and chloride concentrations were 97 ± 1, 14.1 ± 0.02, 2.00 ± 0.04 and 21 ± 0.2 mg $L^{-1}$, respectively, whereas phosphate, ammonium, nitrite and potassium were below the analytical range (< 0.05, < 0.05, < 0.02 and < 5.0 mg $L^{-1}$, respectively).

# 1.12 Metabarcoding-based distribution of *Nitzschia eclipsis*

BLAST searches of 41 metabarcoding datasets from all continents except Australia (Supplementary Data S4 online) revealed exact matches to the 263-bp *rbc*L fragment of D.LDZ5 in only two samples out of more than 11,000 surveyed. Both came from Spain, from (1) the Riu Algars near Batea, Catalunya (Agència Catalana de l'Aigua site code E1060000: UTM 266404, 4552773), and (2) the Río Adra catchment, downstream of the Fuentes de Marbella springs, Almería (Ministerio para la Transición Ecológica y el Reto Demográfico, REFCON, ma016r: UTM 498122, 4074368). The rivers are classified respectively as types RT09 (Mediterranean rivers of variable flow; karstic) and RT10 (Mediterranean rivers with karstic influence); the samples were taken on 20/05/2024 and 20/05/2025. Another ASV, differing by 1 bp from *N. eclipsis* LDZ5 (Supplementary Data S7 online), was detected in the same Riu Algars sample as above but also in small numbers of reads at one site in each of seven US states (Georgia, Missouri, Montana, Nebraska, New Mexico, North Dakota and Wyoming: dataset of Bioproject PRJNA1086463), described by Smucker et al. [44]. Pebble Scout searches of metagenomic and metabarcoding datasets published in NCBI through the end of 2023, using D.LDZ5 *rbc*L, *psb*C and SSU sequences as queries (trimmed to the short region used for metabarcoding to avoid false positives from less variable regions of the genes), gave no exact matches. These detections should be regarded as candidate occurrences of the *Nitzschia eclipsis* lineage rather than confirmed records of the species, because a match to this short barcode fragment does not establish species identity.

## Discussion

# 1.13 Type material and the challenge of linking diatom names to molecular lineages

Historical diatom names are often based on illustrations or permanent preparations that do not reveal all the characters now needed to distinguish morphologically similar species. Re-examination of original material is therefore essential, where it is available, and, where appropriate, lectotypification or epitypification can clarify the application of a name. The epitypification of *Pseudostaurosira polonica* (M.Witak & Lange-Bertalot) E.A.Morales & M.B.Edlund, 2003 illustrates the value of documenting a modern population by LM and SEM when the original material appears to be unavailable and its morphology was incompletely recorded [45]. A further challenge is to connect a name established through morphology to a molecular lineage. Culture-derived epitypes that connect preserved material, documented morphology and DNA sequences offer one way to establish this link [46]. The recent epitypification of *Cocconeis scutellum*, based on a documented cultured strain with associated 18S V4 and *rbc*L sequences, provides another example [47]. Conversely, reference sequences that cannot be traced to documented specimens may be difficult to verify taxonomically, limiting their value for identifying environmental sequences [48].

For *N. archibaldii*, the epitype and SEM observations of material from the same gathering provide a morphological and ultrastructural reference against which other populations can be compared. This reference may also help assess the identity of cultured strains. Rimet et al. [49]. compared LM and SEM

observations with metabarcoding of the same river samples and inferred environmental *rbc*L sequences for morphologically identified diatoms, including *Epithemia hirudiniformis* (O. Müller) Rimet, D.G. Mann, R. Trobajo, J. Zimmermann & R. Jahn, 2018. Mora et al. [50] used a similar approach to infer environmental 18S V4 barcodes for *Iconella delicatissima* (F.W.Lewis) Ruck & Nakov, 2016 and *Navicula notha* J.H.Wallace, 1960. A similar approach could now be explored for *N. archibaldii*: SEM-confirmed occurrences in environmental samples could be assessed alongside *rbc*L ASVs from the same samples to identify candidate barcodes. Metabarcoding does not, however, directly link an ASV to an identified valve. Where morphologically similar *Nitzschia* species and related ASVs co-occur, even a common, SEM-confirmed morphotype and a prominent ASV cannot automatically be equated. Kochorska et al. [51] encountered this difficulty when they could not reliably match similar *Nitzschia* morphotypes with environmental ASVs; Mora et al. [50] also showed that read abundances may differ substantially from valve counts. No reference sequence can currently be assigned unequivocally to *N. archibaldii*. Nevertheless, this species has been reported from samples with both microscopic counts and metabarcoding data [52–54]. In the Hungarian oxbow-lake samples studied by Bíró et al. [18, 53], the nearest environmental ASV differed from *N. eclipsis* by 11 bp in our comparison. This observation does not identify a barcode for *N. archibaldii*, but shows that no *N. eclipsis*-like ASV was detected in those samples. Paired morphological and molecular data may thus help narrow the candidate ASVs for *N. archibaldii*, although any assignment would remain provisional.

## 1.14 Taxonomic distinction of *Nitzschia eclipsis* from *Nitzschia archibaldii*

*Nitzschia archibaldii* was originally described from an unpolluted creek near Bad Homburg, Germany, where it occurred on crusts of the cyanobacterium *Phormidium* [18]. The species has narrow, lightly silicified, lanceolate valves with striae unresolved in LM and no distinctly wider spacing of the median fibulae. Lange-Bertalot distinguished it from *N. paleacea* (Grunow) Grunow, 1881 by the absence of a central nodule and from taxa of the *N. palea* complex by its finer striation. He also noted that it had frequently been reported under incorrect names, most commonly as *N. kuetzingiana* Hilse, 1861 [18]. *N. archibaldii* may be confused with *N. paleacea*, small forms of the *N. palea* complex and other fine-striated *Lanceolatae*-like taxa. Consequently, morphology-based records may include other superficially similar taxa, obscuring the true distribution and ecological preferences of *N. archibaldii* [18–20]. This history of morphological confusion made comparison of the Bogdałów population with the holotype and epitype of *N. archibaldii* particularly important.

The provisional identification of *Nitzschia eclipsis* as *N.* cf. *archibaldii* reflected their close resemblance in LM and the overlap between their published morphometric ranges. *Nitzschia archibaldii* was originally described as 15–40 µm long and 2.5–3.0 µm wide, with 14–19 fibulae and 48–55 striae in 10 µm [18]. Subsequent floras broadened the width to 2–3 µm and the stria density to 46–55 in 10 µm [19, 20]. The published ranges overlap in valve dimensions and fibula density. However, the epitype valves measured here (13.8–21.8 µm; n = 20) do not overlap in length with the examined valves of *N. eclipsis*, although the original length range reported for *N. archibaldii* includes them. Stria density overlaps the range given in

later floras only at 46–47 in 10 µm. Published morphometric ranges therefore do not provide a reliable distinction on their own; valve outline, fibula spacing and ultrastructure are more informative.

Comparison of the holotype slide with *N. eclipsis* reveals subtle differences in valve outline: *N. archibaldii* tapers towards slightly produced, acutely rounded and occasionally weakly capitate apices, whereas *N. eclipsis* tapers more gradually towards narrowly rounded apices. Fibulae are also less regularly spaced in *N. archibaldii*, consistent with the protologue, although the two median fibulae are not separated by a wider gap; in *N. eclipsis*, they are more evenly spaced throughout the valve [18].

Ultrastructure provides clearer separation. Because no unmounted material from the original gathering was available for SEM, the comparison draws on the TEM micrographs published in the protologue and SEM observations of sample 4794 HA and the two additional French populations (Lange-Bertalot, [18], pl. 7, Figs. 115–121). Samples 1189 HA and 1721 HA confirm the characters observed in sample 4794 HA and provide further details of the raphe canal, girdle bands and internal valve structure. The protologue TEM images confirm the weakly capitate apices observed in LM (pl. 7, Figs. 116–118). More importantly, the terminal raphe fissures of *N. archibaldii* appear essentially straight and terminate shortly beyond the last fibula, as shown on pl. 7, Figs. 116, 119. The French specimens similarly have short, only weakly hooked terminal fissures. In *N. eclipsis*, by contrast, the terminal fissures are elongate and strongly recurved, sometimes turning through nearly 180°. Both taxa possess an internal terminal helictoglossa, but only in *N. eclipsis* does the strongly recurved external fissure surround a conspicuous apical siliceous flap. No comparable structure is evident in either the protologue TEM images or the French material of *N. archibaldii*. Laterally tapered girdle-band endings were observed in *N. eclipsis* and in the additional French populations of *N. archibaldii*. The valvocopula bears one longitudinal row of poroids in *N. eclipsis*, compared with two rows documented in those additional populations. In some valves of *N. eclipsis*, the virgae appear slightly raised relative to the adjacent areolate areas. This subtle relief was not observed in the examined French *N. archibaldii* material, where the valve face appears uniformly flat. Because it is not evident in every valve of *N. eclipsis*, we regard it as a supplementary rather than an independently diagnostic character (Supplementary Table S8 online).

# 1.15 Comparison with other morphologically similar taxa

Given the close resemblance between *Nitzschia eclipsis* and *N. archibaldii, N. paleacea* is an important additional comparator because Lange-Bertalot [18] regarded it as the species morphologically closest to *N. archibaldii*. Later accounts report valves 8–55 µm long and 1.5–4 µm wide, with 14–19 fibulae and 44–55 striae in 10 µm, so that its reported morphometric ranges overlap those of both *N. archibaldii* and *N. eclipsis* [20]. Unlike these species, however, *N. paleacea* has central raphe endings (reflected in the presence of a central nodule visible in LM and a distinctly wider gap between the median fibulae), whereas both *N. archibaldii* and *N. eclipsis* lack them [18–20]. The wider median interspace provides a useful LM distinction between *N. eclipsis* and *N. paleacea*, despite the otherwise overlapping morphometrics (Supplementary Table S8 online).

*Nitzschia palea* var. *debilis* (Kützing) Grunow, 1880 should also be considered because it has historically been compared with *N. archibaldii* but generally differs in having broader valves and a lower stria density [18, 20]. *Nitzschia pumila* Hustedt, 1954 is similar to *N. eclipsis* in valve width and fibula density but has longer valves. Krammer and Lange-Bertalot [19] described it as 30–37 µm long and 2.5–3 µm wide, with 14–18 fibulae in 10 µm, but its distinctly elongate, weakly capitate apices contrast with the gradually tapering, non-protracted apices of *N. eclipsis*. Lange-Bertalot and Krammer [55] noted that the smallest specimens of *Nitzschia mediocris* Hustedt, 1949 resemble *N. archibaldii*. Nevertheless, *N. mediocris* is usually 40–50 µm long; even the unusually small specimen illustrated by those authors measured approximately 30 µm, and its stria density was considered to exceed 50 in 10 µm. These measurements separate it from *N. eclipsis* [55]. Other narrow *Lanceolatae*-like taxa illustrated in European floras, such as *N. paleaeformis* Hustedt, 1950 and *N. perminuta* Grunow, 1881, are more readily distinguished from *N. eclipsis* by coarser striation, valve dimensions and apex morphology. *N. paleaeformis* additionally has a wider central interspace between the median fibulae [20] (Supplementary Table S8 online).

# 1.16 Phylogenetic position and morphological comparison within clade 6B

The concatenated SSU–*rbc*L–*psb*C phylogeny places *N. eclipsis* among the finely striated species of clade 6B sensu Mann et al. [7]. The two strains form a maximally supported lineage sister to a strongly supported group comprising *N.* cf. *ardua* L44, *Nitzschia* sp. SZCZCH1090 and *N. excavata* in one subclade, and *N. pusilla* TA420 and TA-45 together with *N. lembiformis* R2 in the other. In the *rbc*L-only tree, *N. eclipsis* is sister to the first of these subclades, which also contains *N. communis* TCC853, but this relationship has low support (UFBoot = 64). Thus, the precise relationships among these lineages remain uncertain.

In both trees, the branch leading to *N. eclipsis* is relatively long, and *N. excavata* is not recovered as its immediate sister taxon in the concatenated analysis. Nevertheless, the two species coexist in Bogdałów reservoir and share several morphological features: linear-lanceolate shape, no central raphe endings and no wider central fibula interspace, similarly dense striation and fibula spacing (44–47 versus 46–49 striae and 12–19 versus 15–22 fibulae in 10 µm, respectively), a tendency for local reduction of the vimines (to create transapically elongate areolae), two rows of areolae in the raphe canal walls, and hooked terminal fissures. A readily visible difference is the larger size of *N. excavata*: its valves are 29.0–50.3 µm long and 3.0–4.4 µm wide, compared with 22–26 µm and 2.0–3.0 µm in *N. eclipsis*. Its apices are also more produced and slightly subcapitate (Supplementary Table S8 online, Supplementary Figure S9 online) [9].

Other taxa in the phylogenetic neighbourhood of *N. eclipsis* differ from it more clearly in valve morphology. The strain identified as *N.* cf. *ardua* has smaller, more linear-elliptical valves and lacks the distinct interruption at the distal valve face–mantle junction observed in *N. eclipsis* [9, 56]. Two other species, *N. communis* and *N. lembiformis*, are also linear-elliptical, with rounded apices, and the distal margin bears a well-marked ridge, rather than having striae interrupted at the valve face–mantle junction

[7, 57, 58]. The valve of *N. pusilla* TA420 illustrated by An et al. ([59], Fig. 3u) is also linear-elliptical; its resemblance to a smaller, very finely striated *N. communis* is based on our unpublished observations. The widely separated positions of strains assigned to *N. pusilla* in molecular trees further indicate that identifications under this name require reassessment. Apart from *N. excavata*, the only member of the clade that has the linear-lanceolate shape of *N. eclipsis* is *Nitzschia* sp. SZCZCH1090, which has elongate valves with distinctly capitate apices and originated from a brackish Baltic habitat, contrasting with the narrow, gradually tapering outline of *N. eclipsis* and its freshwater origin [9]. The phylogenetic neighbourhood of *N. eclipsis* therefore includes contrasting valve morphologies and taxa from both freshwater and brackish habitats. Among the taxa for which ultrastructure has been documented, absence of central raphe endings and two longitudinal rows of poroids in the raphe canal wall are recurrent features; neither character is restricted to this group within clade 6B. On the evidence currently available, no morphological character or combination of characters uniquely diagnoses this phylogenetic neighbourhood [7, 9].

The epitype population of *Nitzschia archibaldii* and the two additional French populations identified here as this species provide ultrastructural evidence for evaluating its possible affinity to clade 6B. Although individual characters are often homoplastic, the combined structure of the raphe canal and girdle bands can retain phylogenetic signal [7]. Relevant features of *N. archibaldii* include uniseriate striae composed of simple poroids and one or locally two longitudinal rows of poroids on the raphe canal wall. The two rows of poroids on the valvocopulae documented in the two additional French populations also occur in some superficially similar members of clade 6B, whereas taxa in clades 8A and 8B generally have a single row or lack poroids on the first girdle band [7]. The lateral, obliquely tapered band endings observed in *N. eclipsis* and in the additional French material of *N. archibaldii* resemble the short bands (*copulae abbreviatae*) described by Mann et al. [60]. Such bands have been documented in several members of clade 6B, including *N. paleacea, N. palea* and *N. eclipsis*, but their full distribution within the clade remains incompletely known. The absence of central raphe endings provides little additional evidence because this condition varies within clade 6B. Together, these features are more consistent with an affinity to clade 6B than to clades 8A or 8B, but none is exclusive to it. The position of *N. archibaldii* must therefore remain tentative until molecular data from unequivocally identified material become available.

# 1.17 Evolutionary signal and hidden diversity in morphologically similar diatoms

The sections of *Nitzschia* established by Cleve and Grunow [8] relied largely on characters visible in LM, including valve outline, symmetry, raphe position and fibula arrangement. Electron microscopy broadened the study of diatom frustule ultrastructure [61], including poroids and details of the raphe canal and girdle bands in *Nitzschia* [18, 57, 60]. Molecular phylogenies then allowed morphological similarities to be assessed in an evolutionary context [6, 7, 62]. At higher taxonomic levels, similar valve structures also need not indicate recent common ancestry. Molecular analyses place species traditionally assigned to *Nitzschia* in several distinct lineages, with other bacillariacean genera nested

among them [7]. Similarly, analyses of *Cymbellales* rejected the then-current circumscription of *Cymbellaceae* under their taxon sampling [63], while tests in *Fragilariaceae* challenged three recent genus circumscriptions [64]. Mapping valve characters onto the latter phylogeny also suggested ancestral retention for some character states and repeated evolution for others [64]. At a broader scale, phylogenomics exposed conflicts with established higher-level classifications and provided the backbone for a classification that recognises monophyletic groups [65, 66]. Shared morphological characters must therefore be evaluated as possible synapomorphies, retained ancestral states or homoplasies before they are used to infer close relationships.

At the species level, these methods address two linked questions: which lineages are distinct, and which historical names apply to them. In the *Sellaphora pupula* complex, morphometrics and reproductive barriers supported the recognition of six demes as separate species, although SEM added few diagnostic characters. Comparison with the lectotype and epitypification linked the name *S. pupula* to the ‘neat’ deme [67]. In the *Achnanthidium minutissimum* (Kützing) Czarnecki, 1994 complex, re-examination of type material clarified the application of several historical names and supported the description of two new species [68]. Within the same complex, however, Dani et al. [69] found broad agreement between SEM identifications, molecular lineages and growth responses, but strains identified as *A. jackii* Rabenhorst, 1861 and *A.* cf. *microcephalum* were not separated by the molecular or ecophysiological data. Other complexes reveal limits that persist even when additional markers or more detailed microscopy are used. Within *Nitzschia palea*, molecular and mating patterns did not align with the traditional distinction between var. *palea* and var. *debilis* [70]. Estimates of molecular operational taxonomic unit (MOTU) diversity depended on marker choice and sequence-similarity thresholds and remained constrained by geographical sampling [71]. Phylogenomic analysis subsequently found discordance among gene trees consistent with incomplete lineage sorting and inferred gene flow between lineages, including a putative hybrid [72]. A different limit is evident in *Pinnularia borealis* Ehrenberg, 1843, LM morphometrics of 70 clones and SEM examination of selected strains revealed subtle differences among eight molecular lineages, but no characters that reliably identified individual valves. The terms “cryptic” and “pseudocryptic” therefore describe how readily lineages can be distinguished morphologically; they do not, by themselves, identify the processes responsible for their divergence [73]. Within clade 6B of *Nitzschia*, *N. excavata* illustrates how close resemblance in LM can give a misleading impression of relationship. Its valves resemble those of *N. palea*, but closer examination reveals differences in striation and fibula arrangement, and a three-marker phylogeny places the two species in distinct, non-sister lineages [9]. *Nitzschia captiva* and *N. agnita* are remarkably similar in valve morphology but differ in girdle structure; examining type material was important in resolving their identities [74]. Although *N. captiva* belongs to clade 6B, the absence of sequences for *N. agnita* prevents a direct test of their relationship. Our comparisons highlight terminal raphe architecture, the valve face–mantle transition, raphe-canal ornamentation and valvocopula structure as candidate characters for species delimitation and phylogenetic interpretation within clade 6B. Testing them across a broader range of sequenced taxa is needed to determine which character combinations carry a consistent phylogenetic signal [7]. Short girdle bands also occur in other clade 6B species with different

valve morphologies, suggesting that girdle structure, valve morphology, or both have evolved convergently [74].

By anchoring the name *N. archibaldii* to an epitype and linking the morphology of the Bogdałów population to a multigene lineage, our study addresses a recurrent difficulty in identifying similar-looking diatoms: specimens that are hard to separate confidently in LM may represent distinct species. SEM provides a morphological basis for distinguishing *N. eclipsis* from *N. archibaldii*, while the phylogeny establishes *N. eclipsis* as a distinct lineage among the sequenced members of clade 6B. The identity of the Bogdałów population and the morphological application of the name *N. archibaldii* are thus clarified, although the relationship between the two species remains unresolved because no sequence can yet be assigned securely to *N. archibaldii*.

# 1.18 Molecular traces beyond the type locality

When morphologically similar species are identified under a single name, microscopy-based records cannot show their individual distributions. Once well-supported species concepts have been linked to reliable reference sequences, it becomes possible to retrospectively screen ASV libraries for matches that suggest occurrences beyond the type locality and associate them with recorded environmental conditions [9, 75, 76]. However, because the commonly used *rbc*L metabarcode is relatively short, even exact matches may not represent the target species, since closely related taxa sometimes share the same barcode [9, 75]. Such records should therefore be treated as evidence of the potential environmental distribution of a lineage, rather than unequivocal species-level records. Once enough datasets become available, long-read metabarcoding using full-length *rbc*L, or full *rbc*L–*rbc*S sequences (given that these genes are apparently always syntenic in diatoms, e.g. Wang et al. [77]) will offer the possibility of more definitive conclusions.

Our survey of available metabarcoding datasets (Supplementary Data S4, S7 online) shows that the *N. eclipsis* lineage may occur elsewhere. Exact matches to the Polish *N. eclipsis* isolates were found in two Spanish samples; if an ASV differing by one bp also represents the species, *N. eclipsis* is also widely distributed in the USA. So far, however, the number of known sites is small and nowhere is it abundant. The small number of records does not, by itself, establish a restricted geographical range. Nevertheless, metabarcoding or metagenomics approaches are a practical way to investigate the geographical and ecological range of *N. eclipsis*, given the difficulty in separating it from *N. archibaldii* in LM, or indeed in SEM. For the moment, all that can be said is that the three known sites with exact matches to *N. eclipsis* *rbc*L are alkaline or karstic.

The other species described from Bogdałów illustrate why the number of molecular records should be interpreted cautiously. Published searches found exact or closely related sequences of *N. excavata* at distant sites in Europe and China [9], whereas metabarcoding extended the recorded distribution of *N. nandorii* to other parts of Europe, California and Ontario [75]. Preliminary, unpublished *rbc*L metabarcoding of bromeliad-associated samples from Colombia also yielded a 263-bp ASV identical to the *N. excavata* reference across the analysed fragment. These records show that discovery in a post-

mining reservoir does not imply geographical restriction; differences in the number of detections cannot yet be equated with differences in the species' actual ranges.

An extra point emerging from our distributional study is that polluted systems resulting from past industrial activity and newly restored environments should not be assumed to lack taxonomic interest, relative to more pristine habitats, especially because unusual conditions may be created that select for species that are otherwise rare. *Nitzschia eclipsis* is a clear example of a species that is infrequently detected, at least in the lakes, rivers and streams included so far in metabarcoding studies. In three Czech post-mining lakes, 25% of the diatom species recorded in the surrounding watershed were found only in those lakes [78]. Taxonomic exploration of a wider range of habitats is needed to explore the full diversity of diatoms in freshwaters and to obtain reference material for sequence databases. Mine pit lakes and other post-mining waters remain underrepresented in research on freshwater microorganisms, and existing studies have generally focused largely on water chemistry and highly acidic systems [79]. Circumneutral and alkaline post-mining reservoirs may therefore harbour overlooked lineages lacking reliable morphological concepts and reference sequences.

## Conclusions

The epitype, together with SEM observations of other valves from the same gathering, clarifies the morphological application of the name *Nitzschia archibaldii*. Against this reference, the Bogdałów population is diagnosable as *N. eclipsis*, and its two cultured strains form a maximally supported lineage among sequenced members of clade 6B. This illustrates pseudocryptic diversity: the species boundary is difficult to recognise reliably in routine light microscopy, so records based on similar valve outlines may combine distinct species and obscure their individual distributions. The phylogenetic relationship between *N. eclipsis* and *N. archibaldii* cannot be tested directly in the present molecular phylogeny because no sequence can be assigned unequivocally to *N. archibaldii*, while the phylogenetic significance of the diagnostic ultrastructural characters requires broader sampling. Among more than 11,000 metabarcoded samples, exact matches to the short *N. eclipsis rbc*L fragment occurred in only two, both from Spain; a one-base variant was also found in the United States. These geographically distant matches suggest occurrences beyond Bogdałów, but neither define the species' range nor demonstrate that it is rare. The case shows how a post-mining reservoir can harbour an overlooked evolutionary lineage and how resolving its identity can open new questions about the evolution of valve characters and the distribution of finely striated *Nitzschia*.

## Declarations

# Competing interests

The authors declare no competing financial interests or personal relationships that could have influenced the work reported in this manuscript.

# Funding

Declaration

This research was supported by the National Science Centre, Poland, under the MINIATURA 10 call (grant no. 2026/10/X/NZ8/00048). R.M.O. was additionally supported by the Polish National Agency for Academic Exchange (NAWA) under the Bekker NAWA Programme (grant no. BPN/BEK/2025/1/00107/U/00001).

# Author Contribution

RMO: Conceptualisation, Methodology, Formal analysis, Investigation, Resources, Data curation, Visualisation, Writing – original draft, Writing – review & editing, Project administration, Funding acquisition.DGM: Conceptualisation, Formal analysis, Investigation, Resources, Data curation, Writing – original draft, Writing – review & editing.RT: Conceptualisation, Formal analysis, Investigation, Resources, Data curation, Writing – review & editing.PKZ: Methodology, Formal analysis, Investigation, Writing – review & editing.JS: Investigation, Resources, Visualisation, Writing – review & editing.ŁP: Methodology, Investigation, Visualisation, Writing – review & editing.CEW: Methodology, Investigation, Visualisation, Writing – review & editing.MG: Methodology, Investigation, Visualisation, Writing – review & editing.EG: Investigation, Visualisation, Writing – review & editing.JZW: Data curation, Writing – review & editing.

# Acknowledgement

We thank Prof. Horst Lange-Bertalot, Andrew Charles Podzorski (Diatoms, Senckenberg Research Institute and Natural History Museum Frankfurt), and Dr Nélida Abarca (Curator, Algae Herbarium, Botanischer Garten Berlin) for their assistance in searching for type material of Nitzschia archibaldii. David Heudre (LIST) is thanked for his technical assistance with microscopy imaging (virtual slide) of Nitzschia archibaldii slide.We gratefully acknowledge Polish high-performance computing infrastructure PLGrid (HPC Center: CI TASK) for providing computer facilities and support within computational grant no. PLG/2026/019954The Royal Botanic Garden Edinburgh is supported by the Scottish Government's Rural and Environment Science and Analytical Services Division and IRTA receives support from the CERCA Programme/ Generalitat de Catalunya.The UK metabarcoding data searched in this paper here were generated and provided by the Environment Agency of England (see also Kelly et al. 2024): we are most grateful to Dr Kerry Walsh for making the data available. Drs Emilie Lyautey and Stéphane Pesce made available to us the raw fastq files for BioProject PRJEB85099 (Rogue et al., 2025), and Prof. Xudong Liu sent us the raw files for a metabarcoding study of urban rivers in Zhejiang Province, E China (Wang et al., 2024). These two datasets were included in the compilation we searched for records of N. eclipsis: we are very grateful to both groups for their help, although neither dataset proved to contain the new species.

# Data Availability

The sequences generated in this study have been deposited in GenBank under accession numbers PZ871626 (SSU rDNA), PZ881546–PZ881547 (rbcL), and PZ881544–PZ881545 (psbC). Nitzschia eclipsis is registered in PhycoBank under number 107763; the epitype of Nitzschia archibaldii is registered under number 107820, and a digital scan of its slide is available at https://doi.org/10.5281/zenodo.22896583. The sequence-accession dataset is provided as Supplementary Data S2 online, and the alignment and phylogenetic files as Supplementary Data S3 online. The compiled metabarcoding dataset and the alignment of the reference rbcL fragment with matching ASVs are provided as Supplementary Data S4 online and Supplementary Data S7 online, respectively.

# References


1. Mann, D. G. The species concept in diatoms: Evidence for morphologically distinct, sympatric gamodemes in four epipelic species. *Plant Syst. Evol.* **164**, 215–237 (1989).
2. Mann, D. G. The species concept in diatoms. *Phycologia* **38**, 437–495 (1999).
3. Abarca, N., Jahn, R., Zimmermann, J. & Enke, N. Does the Cosmopolitan Diatom *Gomphonema parvulum* (Kützing) Kützing Have a Biogeography? *PLoS One*. **9**, e86885 (2014).
4. Evans, K. M., Wortley, A. H., Simpson, G. E., Chepurnov, V. A. & Mann, D. G. A molecular systematic approach to explore diversity within the *Sellaphora pupula* species complex (Bacillariophyta). *J. Phycol.* **44**, 215–231 (2008).
5. Vanormelingen, P., Chepurnov, V. A., Mann, D. G., Cousin, S. & Vyverman, W. Congruence of morphological, reproductive and ITS rDNA sequence data in some Australasian *Eunotia bilunaris* (Bacillariophyta). *Eur. J. Phycol.* **42**, 61–79 (2007).
6. Rimet, F. et al. Molecular phylogeny of the family Bacillariaceae based on 18S rDNA sequences: Focus on freshwater *Nitzschia* of the section Lanceolatae. *Diatom Res.* **26**, 273–291 (2011).
7. Mann, D. G. et al. Ripe for reassessment: A synthesis of available molecular data for the speciose diatom family Bacillariaceae. *Mol. Phylogenet Evol.* **158**, 106985 (2021).
8. Cleve, P. T. & Grunow, A. Beiträge zur Kenntniss der arctischen Diatomeen. *Kongliga Svenska Vetenskaps-Akademiens Handlingar*. **17**, 1–121 (1880).
9. Olszyński, R. M. et al. *Nitzschia excavata* sp. nov. (Bacillariaceae), a new diatom species from a post-mining reservoir revealed by morphology, molecular phylogeny, and metabarcoding-based biogeography. *Sci. Rep.* **16**, 16561 (2026).
10. Olszyński, R. M. et al. Morphology and phylogeny of *Nitzschia nandorii* sp. nov. (Bacillariophyceae), a new small-celled lanceolate species from a post-mining reservoir. *PhytoKeys* **241**, 1–26 (2024).
11. Olszyński, R. M., Szczepocka, E. & Żelazna-Wieczorek, J. Critical multi-stranded approach for determining the ecological values of diatoms in unique aquatic ecosystems of anthropogenic origin. *PeerJ* **7**, e8117 (2019).

12. Orlikowski, D. & Szwed, L. Wodny kierunek rekultywacji w KWB „Adamów SA – inwestycją w przyszłość regionu. *Górnictwo i Geoinżynieria*. **33**, 351–361 (2009).
13. Orlikowski, D. & Szwed, L. Zagospodarowanie terenów pogórniczych KWB „ADAMÓW SA w Turku  krajobraz przed rozpoczęciem działalności górniczej i po jej zakończeniu. *Górnictwo i Geoinżynieria*. **35**, 225–240 (2011).
14. Stachowski, P. Rekultywacja wodna na zdewastowanych obszarach pogórniczych Wschodniej Wielkopolski jako element ich zagospodarowania. *Space – Soc. – Econ.* **35**, 125–143 (2024).
15. Stachowski, P., Kraczkowska, K., Liberacki, D. & Oliskiewicz-Krzywicka, A. Water Reservoirs as an Element of Shaping Water Resources of Post-Mining Areas. *J. Ecol. Eng.* **19**, 217–225 (2018).
16. Baricevic, A. et al. Recommendations for the preservation of environmental samples in diatom metabarcoding studies. *Metabarcoding Metagenom*. **6**, e85844 (2022).
17. CEN. Water quality—Guidance standard for the routine sampling and preparation of benthic diatoms from rivers and lakes. (2025).
18. Lange-Bertalot, H. New species, combinations and synonyms in the genus *Nitzschia*. *Bacillaria* **3**, 41–78 (1980).
19. Krammer, K. & Lange-Bertalot, H. Bacillariophyceae. 2 Teil: Bacillariaceae, Epithemiaceae, Surirellaceae. in Süsswasserflora von Mitteleuropa (eds Ettl, H., Gerloff, J., Heynig, H. & Mollenhauer, D.) vol 2/2 1–610 (Spektrum, Akad., Jena, (1997).
20. Lange-Bertalot, H., Hofmann, G., Werum, M., Cantonati, M. & Kelly, M. G. *Freshwater Benthic Diatoms of Central Europe: Over 800 Common Species Used in Ecological Assessment* (Koeltz Botanical Books, 2017).
21. Żelazna-Wieczorek, J. A.R.G. Gantner K.G., Ruggell,. Diatom flora in springs of Łódź Hills (Central Poland). Biodiversity, taxonomy, and temporal changes of epipsammic diatom assemblages in springs affected by human impact. in *Diatom Monographs* (ed. Witkowski, A.) vol. 13 1–419 (2011).
22. Dąbek, P. et al. Towards a multigene phylogeny of the Cymatosiraceae (Bacillariophyta, Mediophyceae) I: novel taxa within the subfamily Cymatosiroideae based on molecular and morphological data. *J. Phycol.* **53**, 342–360 (2017).
23. Ruck, E. C. & Theriot, E. C. Origin and Evolution of the Canal Raphe System in Diatoms. *Protist* **162**, 723–737 (2011).
24. Edgar, S. M. & Theriot, E. C. Phylogeny of *Aulacoseira* (Bacillariophyta) based on molecules and morphology. *J. Phycol.* **40**, 772–788 (2004).
25. Kawai, H., Hanyuda, T., Draisma, S. G. A., Wilce, R. T. & Andersen, R. A. Molecular phylogeny of two unusual brown algae, *Phaeostrophion irregulare* and *Platysiphon glacialis*, proposal of the *Stschapoviales* ord. nov. and Platysiphonaceae fam. nov., and a re-examination of divergence times for brown algal orders. *J. Phycol.* **51**, 918–928 (2015).
26. Medlin, L., Elwood, H. J., Stickel, S. & Sogin, M. L. The characterization of enzymatically amplified eukaryotic 16S-like rRNA-coding regions. *Gene* **71**, 491–499 (1988).

27. Yamada, N., Sym, S. D. & Horiguchi, T. Identification of Highly Divergent Diatom-Derived Chloroplasts in Dinoflagellates, Including a Description of Durinskia kwazulunatalensis sp. nov. (Peridiniales, Dinophyceae). *Mol. Biol. Evol.* **34**, 1335–1351 (2017).
28. Imanian, B., Pombert, J. F. & Keeling, P. J. The Complete Plastid Genomes of the Two 'Dinotoms' *Durinskia baltica* and *Kryptoperidinium foliaceum*. *PLoS One*. **5**, e10711 (2010).
29. Yamada, N., Sakai, H., Onuma, R., Kroth, P. G. & Horiguchi, T. Five Non-motile Dinotom Dinoflagellates of the Genus *Dinothrix*. *Front. Plant. Sci.* **11**, 591050 (2020).
30. Katoh, K., Rozewicki, J. & Yamada, K. D. MAFFT online service: multiple sequence alignment, interactive sequence choice and visualization. *Brief. Bioinform*. **20**, 1160–1166 (2019).
31. Kalyaanamoorthy, S., Minh, B. Q., Wong, T. K. F., Von Haeseler, A. & Jermiin, L. S. ModelFinder: fast model selection for accurate phylogenetic estimates. *Nature Methods 2017 14:6* 14, 587–589 (2017).
32. Chernomor, O., Von Haeseler, A. & Minh, B. Q. Terrace Aware Data Structure for Phylogenomic Inference from Supermatrices. *Syst. Biol.* **65**, 997–1008 (2016).
33. Wong, T. K. F. et al. IQ-TREE 3: phylogenomic inference software using complex evolutionary models. *Mol. Biol. Evol.* **43**, 1–6 (2026).
34. Hoang, D. T., Chernomor, O., Von Haeseler, A., Minh, B. Q. & Vinh, L. S. UFBoot2: Improving the Ultrafast Bootstrap Approximation. *Mol. Biol. Evol.* **35**, 518–522 (2018).
35. Guindon, S. et al. New Algorithms and Methods to Estimate Maximum-Likelihood Phylogenies: Assessing the Performance of PhyML 3.0. *Syst. Biol.* **59**, 307–321 (2010).
36. Anisimova, M., Gil, M., Dufayard, J. F., Dessimoz, C. & Gascuel, O. Survey of Branch Support Methods Demonstrates Accuracy, Power, and Robustness of Fast Likelihood-based Approximation Schemes. *Syst. Biol.* **60**, 685–699 (2011).
37. Ronquist, F. et al. MrBayes 3.2: Efficient Bayesian Phylogenetic Inference and Model Choice Across a Large Model Space. *Syst. Biol.* **61**, 539–542 (2012).
38. Letunic, I. & Bork, P. Interactive Tree of Life (iTOL) v6: recent updates to the phylogenetic tree display and annotation tool. *Nucleic Acids Res.* **52**, W78–W82 (2024).
39. Callahan, B. J. et al. DADA2: High-resolution sample inference from Illumina amplicon data. *Nat. Methods*. **13**, 581–583 (2016).
40. Altschul, S. F., Gish, W., Miller, W., Myers, E. W. & Lipman, D. J. Basic local alignment search tool. *J. Mol. Biol.* **215**, 403–410 (1990).
41. Shiryev, S. A. & Agarwala, R. Indexing and searching petabase-scale nucleotide resources. *Nature Methods 2024 21:6* 21, 994–1002 (2024).
42. Heudre, D. & Wetzel, C. E. *Nitzschia archibaldii* Lange-Bertalot 1980. Preprint at (2026). https://doi.org/10.5281/zenodo.22896583
43. Turland, N. J. et al. International Code of Nomenclature for Algae, Fungi, and Plants (Madrid Code). *Regnum Vegetabile* vol. 162University of Chicago Press, Chicago, (2025).

44. Smucker, N. J. et al. Using DNA metabarcoding to characterize national scale diatom-environment relationships and to develop indicators in streams and rivers of the United States. *Sci. Total Environ.* **939**, 173502 (2024).
45. Van de Vijver, B., Cantonati, M., Angeli, N. & Kusber, W. H. Refined morphological circumscription and epitypification of *Pseudostaurosira polonica* (Witak & Lange-Bertalot) E.Morales & Edlund (Staurosiraceae, Bacillariophyta), an overlooked freshwater diatom species in Europe. *Bot. Lett.* 172, 360–365 (2025).
46. Evans, K. M. & Mann, D. G. A proposed protocol for nomenclaturally effective DNA barcoding of microalgae. *Phycologia* **48**, 70–74 (2009).
47. Skibbe, O. et al. Morphomolecular characterization and epitypification of *Cocconeis scutellum* (Bacillariophyceae), type of the diatom genus *Cocconeis*. *Willdenowia* **56**, 185–208 (2026).
48. Zimmermann, J. et al. Taxonomic Reference Libraries for Environmental Barcoding: A Best Practice Example from Diatom Research. *PLoS One*. **9**, e108793 (2014).
49. Rimet, F. et al. The potential of High-Throughput Sequencing (HTS) of natural samples as a source of primary taxonomic information for reference libraries of diatom barcodes. *Fottea* **18**, 37–54 (2018).
50. Mora, D. et al. Morphology and metabarcoding: A test with stream diatoms from Mexico highlights the complementarity of identification methods. *Freshw. Sci.* **38**, 448–464 (2019).
51. Kochoska, H. et al. Filling reference libraries with diatom environmental sequences: strengths and weaknesses. *Diatom Res.* **38**, 103–127 (2023).
52. Duleba, M. et al. Applicability of diatom metabarcoding in the ecological status assessment of Hungarian lotic and soda pan habitats. *Ecol. Indic.* **130**, 108105 (2021).
53. Bíró, T. et al. Metabarcoding as an effective complement of microscopic studies in revealing the composition of the diatom community – a case study of an oxbow lake of Tisza River (Hungary) with the description of a new *Mayamaea species*. *Metabarcoding Metagenom*. **6**, e87497 (2022).
54. Kelly, M. G. et al. Development of a novel metric for evaluating diatom assemblages in rivers using DNA metabarcoding. *Ecol. Indic.* **118**, 106725 (2020).
55. Lange-Bertalot, H. & Krammer, K. *Bacillariaceae, Epithemiaceae, Surirellaceae: Neue Und Wenig Bekannte Taxa, Neue Kombinationen Und Synonyme Sowie Bemerkungen Und Ergänzungen Zu Den Naviculaceae*. *Bibliotheca Diatomologica* vol. 15 (J. Cramer, Berlin; Stuttgart, (1987).
56. Rovira, L., Trobajo, R., Sato, S., Ibáñez, C. & Mann, D. G. Genetic and Physiological Diversity in the Diatom *Nitzschia inconspicua*. *J. Eukaryot. Microbiol.* **62**, 815–832 (2015).
57. Mann, D. G. *Studies in the Nitzschiaceae (Bacillariophyta)* (University of Bristol, 1978).
58. Clavero i Oms, E. Diatomees d'ambient hipersalins costaners. Taxonomia, distribució i em-premtes en el registre sedimentari. (2004). https://dialnet.unirioja.es/servlet/tesis?codigo=255151&info=resumen&idioma=SPA

59. An, S. M., Choi, D. H., Lee, J. H., Lee, H. & Noh, J. H. Identification of benthic diatoms isolated from the eastern tidal flats of the Yellow Sea: Comparison between morphological and molecular approaches. *PLoS One*. **12**, e0179422 (2017).
60. Mann, D. G., Wetzel, C. E. & Trobajo, R. A new type of girdle band in Bacillariaceae. *Nova Hedwig Beih*. **151**, 141–159 (2021).
61. Ross, R. et al. An amended terminology for the siliceous components of the diatom cell. *Nova Hedwigia*. **64**, 513–533 (1979).
62. Lundholm, N., Daugbjerg, N. & Moestrup, Ø. Phylogeny of the Bacillariaceae with emphasis on the genus Pseudo-nitzschia (Bacillariophyceae) based on partial LSU rDNA. *Eur. J. Phycol.* **37**, 115–134 (2002).
63. Nakov, T., Ruck, E. C., Galachyants, Y., Spaulding, S. A. & Theriot, E. C. Molecular phylogeny of the Cymbellales (Bacillariophyceae, Heterokontophyta) with a comparison of models for accommodating rate variation across sites. *Phycologia* **53**, 359–373 (2014).
64. Trentin, R., Moschin, E., Schiaparelli, S. & Moro, I. An insight into the cryptic diversity of Fragilariaceae (Bacillariophyta), with the description of a new Antarctic species, *Gedaniella antarctica* sp. nov. *Eur. J. Phycol.* **59**, 379–392 (2024).
65. Alverson, A. J. et al. Phylogenomics reveals the slow-burning fuse of diatom evolution. *Proc. Natl. Acad. Sci. U. S. A.* 122, e2500153122 (2025).
66. Kociolek, J. P., Ashworth, M. P. & Alverson, A. J. A phylogenetic classification of diatoms (Bacillariophyta). *J. Phycol.* **62**, 44–67 (2026).
67. Mann, D. G. et al. The *Sellaphora pupula* species complex (Bacillariophyceae): morphometric analysis, ultrastructure and mating data provide evidence for five new species. *Phycologia* **43**, 459–482 (2004).
68. Novais, M. H. et al. Morphological variability within the *Achnanthidium minutissimum* species complex (Bacillariophyta): comparison between the type material of *Achnanthes minutissima* and related taxa, and new freshwater *Achnanthidium* species from Portugal. *Phytotaxa* **224**, 101–139 (2015).
69. Dani, M. et al. Species delimitation within the *Achnanthidium minutissimum* complex (Bacillariophyta), based on morphological, molecular, and ecophysiological approaches. *J. Phycol.* **62**, 25–43 (2026).
70. Trobajo, R. et al. Morphological, genetic and mating diversity within the widespread bioindicator Nitzschia palea (Bacillariophyceae). *Phycologia* **48**, 443–459 (2009).
71. Rimet, F. et al. When is Sampling Complete? The Effects of Geographical Range and Marker Choice on Perceived Diversity in *Nitzschia palea* (Bacillariophyta). *Protist* **165**, 245–259 (2014).
72. Çiftçi, O. et al. Phylotranscriptomics reveals the reticulate evolutionary history of a widespread diatom species complex. *J. Phycol.* **58**, 643–656 (2022).
73. Pinseel, E. et al. Extensive Cryptic Diversity in the Terrestrial Diatom < i>Pinnularia borealis < i/> (Bacillariophyceae). *Protist* **170**, 121–140 (2019).

74. Mann, D. G., Yamada, N., Bolton, J. J., Witkowski, A. & Trobajo, R. *Nitzschia captiva* sp. nov. (Bacillariophyta), the essential prey diatom of the kleptoplastic dinoflagellate *Durinskia capensis*, compared with *N. agnita, N. kuetzingioides* and other species. *Phycologia* **62**, 136–151 (2023).
75. Pérez-Burillo, J., Mann, D. G. & Trobajo, R. Biogeography and genetic diversity of freshwater diatoms: The potential of large combined rbcL metabarcoding datasets. *Sci. Total Environ.* **966**, 178727 (2025).
76. Abubaker, B., Stenger-Kovács, C., Rimet, F. & Tapolczai, K. DNA metabarcoding of diatoms: A next-generation tool for aquatic biodiversity and bioassessment. *Metabarcoding Metagenom*. **10**, e168096 (2026).
77. Wang, Y. et al. Comparative Analysis of Bacillariophyceae Chloroplast Genomes Uncovers Extensive Genome Rearrangements Associated with Speciation. *Int. J. Environ. Res. Public. Health 2022*. **19**, 10024 (2022).
78. Bešta, T. et al. Littoral periphyton dynamics in newly established post-mining lakes. *Aquat. Sci.* **85**, 21 (2022).
79. Bernasconi, R., Lund, M. A. & Blanchette, M. L. Non-charismatic waterbodies and ecosystem disservices: Mine pit lakes are underrepresented in the literature. *Front. Microbiol.* **13**, 1063594 (2022).

# Figures




**Figure 1**

*Nitzschia archibaldii* Lange-Bertalot, holotype slide and specimens from the holotype material. (**A**) Original holotype slide with handwritten labels indicating Bad Homburg, Braumanns Wiesen, 1975, and the identification as *N. archibaldii*. (**B–P**) Light microscopy photomicrographs of valves from the holotype slide, showing variation in valve outline and dimensions. Scale bar = 10 µm (B–P).

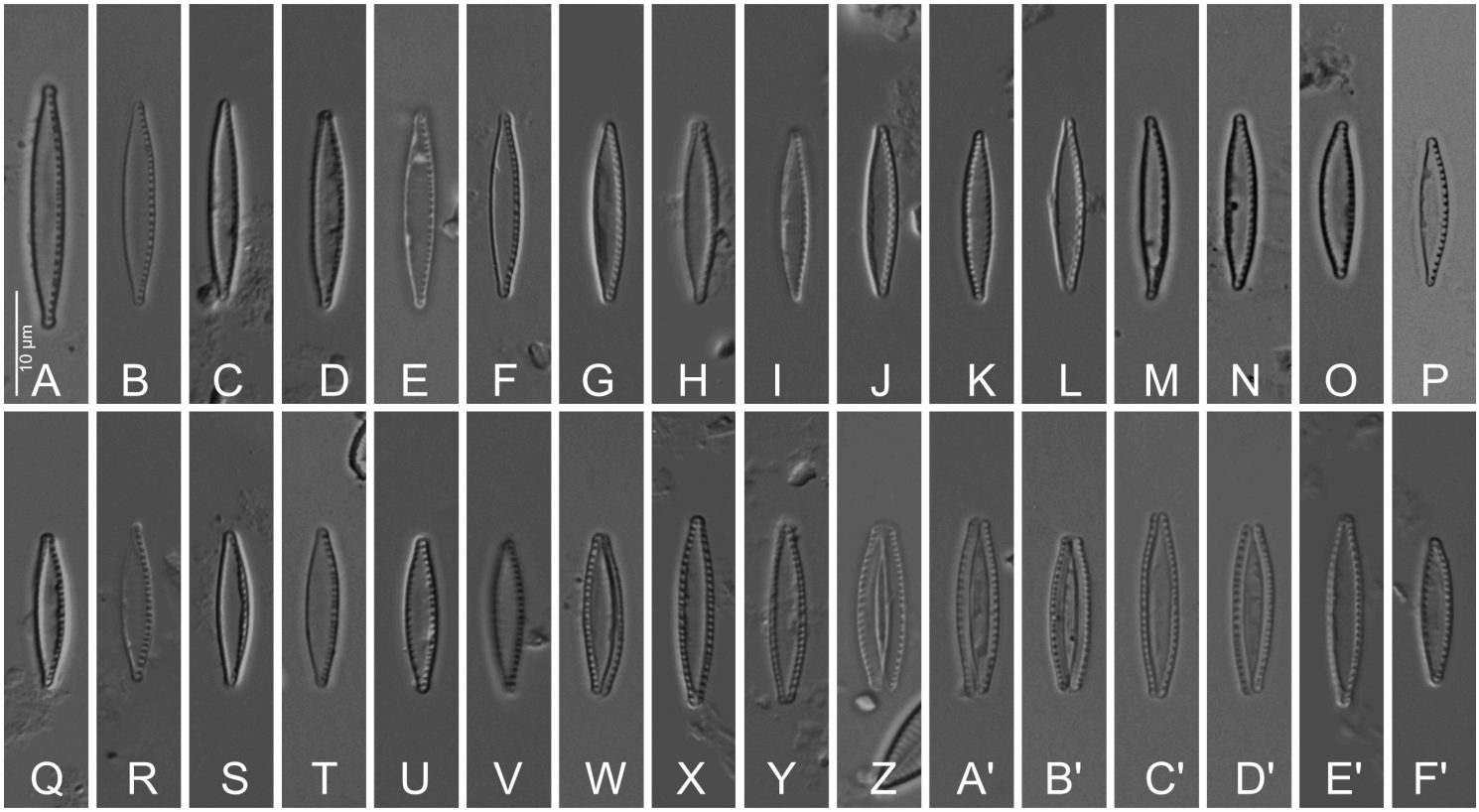



**Figure 2**

Light microscopy photomicrographs of *Nitzschia archibaldii* Lange-Bertalot from the epitype population, sample 4794 HA, collected from the L'Automne River at Bémont, France. (A–F') Variation in valve outline and size. The valve in P is the epitype specimen designated here, located on permanent slide 4794 HA. Scale bar = 10 µm.

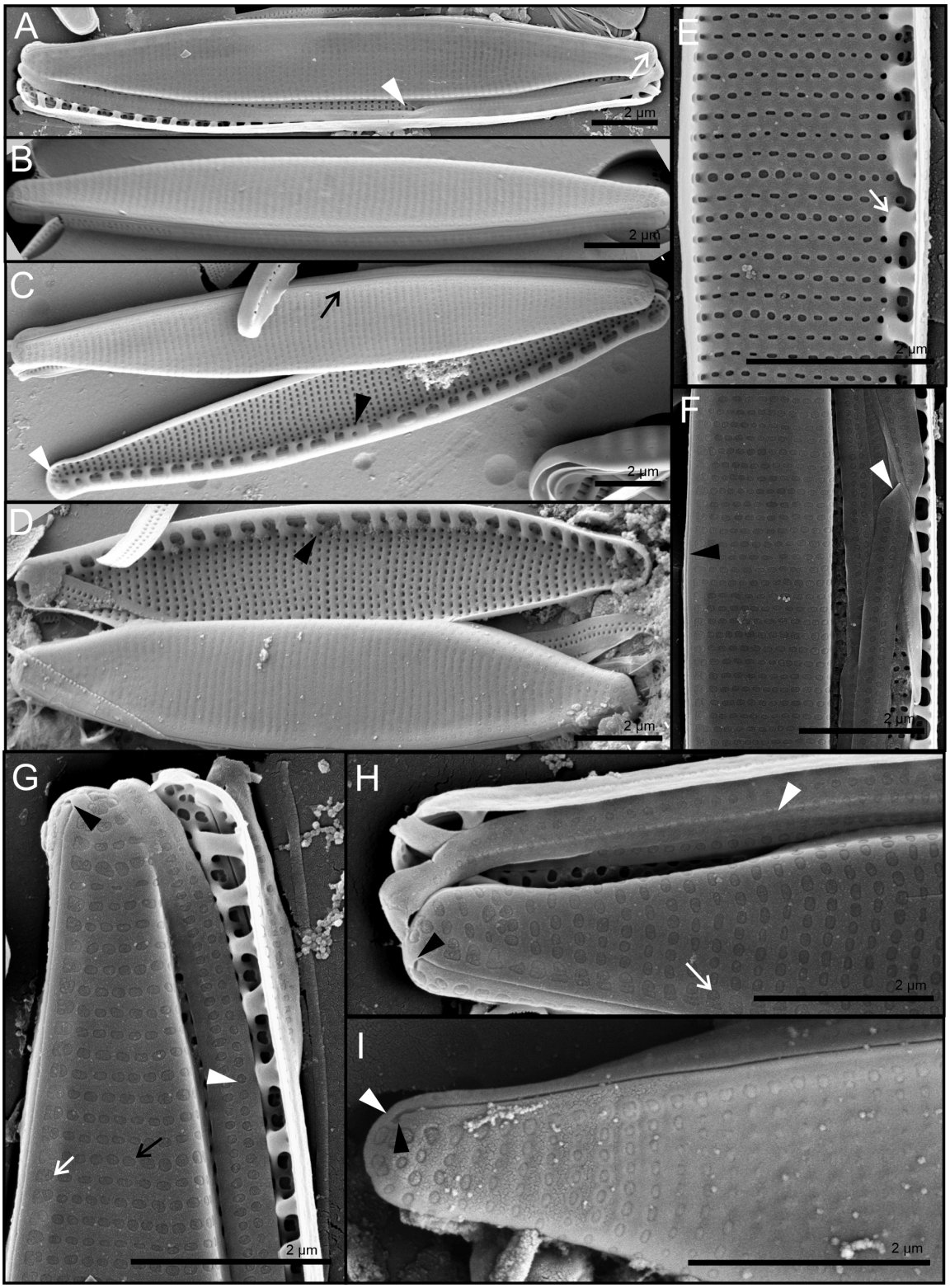



**Figure 3**

Scanning electron microscopy (SEM) micrographs of *Nitzschia archibaldii* Lange-Bertalot from three French populations identified here as this species: sample 1189 HA (**A, E–H**), sample 1721 HA (**B, C**) and sample 4794 HA (**D, I**); epitype gathering. (**A–B**) External views of entire valves with pore occlusions retained. In **A**, the white arrow indicates the short, weakly hooked terminal raphe fissure. Arrowheads indicate that an obliquely tapered lateral end of a girdle band is visible alongside the valve. (**C–D**) Internal

and external views of valves. Internal views show narrow, irregularly spaced fibulae, usually connected to two virgae (black arrowheads); the white arrowhead in **C** indicates a small helictoglossa. In the external view in **C**, the black arrow indicates an uninterrupted raphe. (**E**) Internal detail of the valve and raphe canal; the white arrow indicates a fibula without ornamentation and connecting to two virgae. (**F**) External details of the valve face, raphe canal and valvocopula. The black arrowhead indicates the continuous raphe slit lacking central endings, which is visible along the adjacent valve margin, whereas the white arrowhead marks the end of a valvocopula bearing two longitudinal rows of poroids. Poration diminishes towards this end, suggesting an obliquely tapered termination. (**G–I**) External views of the valve apices. Black arrowheads indicate short, weakly hooked terminal raphe fissures, whereas white arrowheads indicate valvocopulae bearing two longitudinal rows of poroids. White arrows in G–H indicate wider poroids on the raphe canal wall, while the black arrow in G indicates typical valve-face areolae. Scale bars = 2 μm.

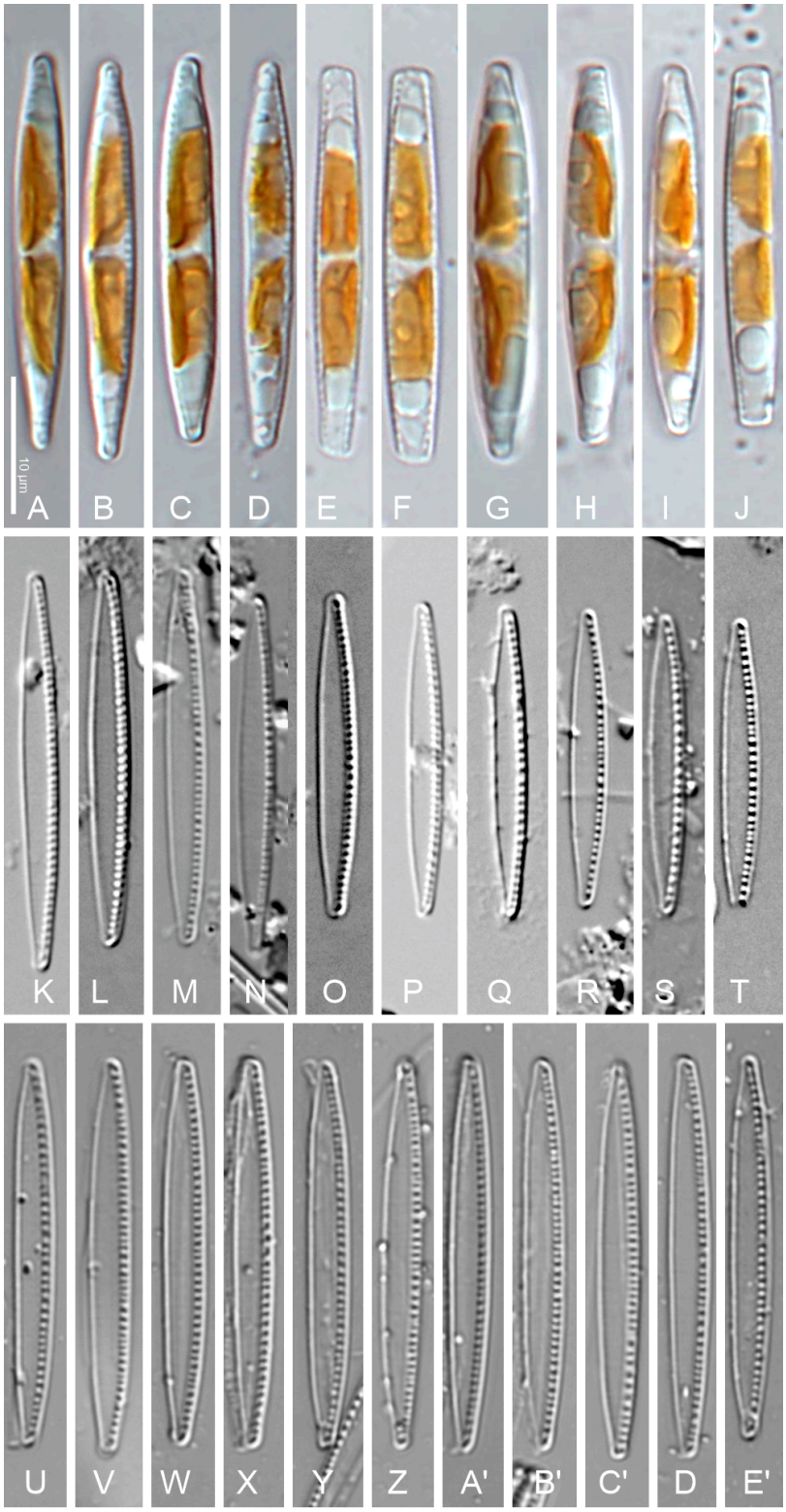



**Figure 4**

Light microscope (DIC) photomicrographs of *Nitzschia eclipsis* sp. nov. (**A–J**) Photomicrographs of living cells from culture material. Representative cells showing two golden-brown plastids arranged longitudinally and occupying opposite halves of the cell and volutin granules at the apex of each chloroplast. (**K–E'**) Light microscopy photomicrographs of *Nitzschia eclipsis* sp. nov. (**K–T**) Valves from

the environmental samples, showing variation in valve outline and dimensions. **M** Holotype specimen. (**U–E'**) Valves from the culture material. Scale bar = 10 μm.

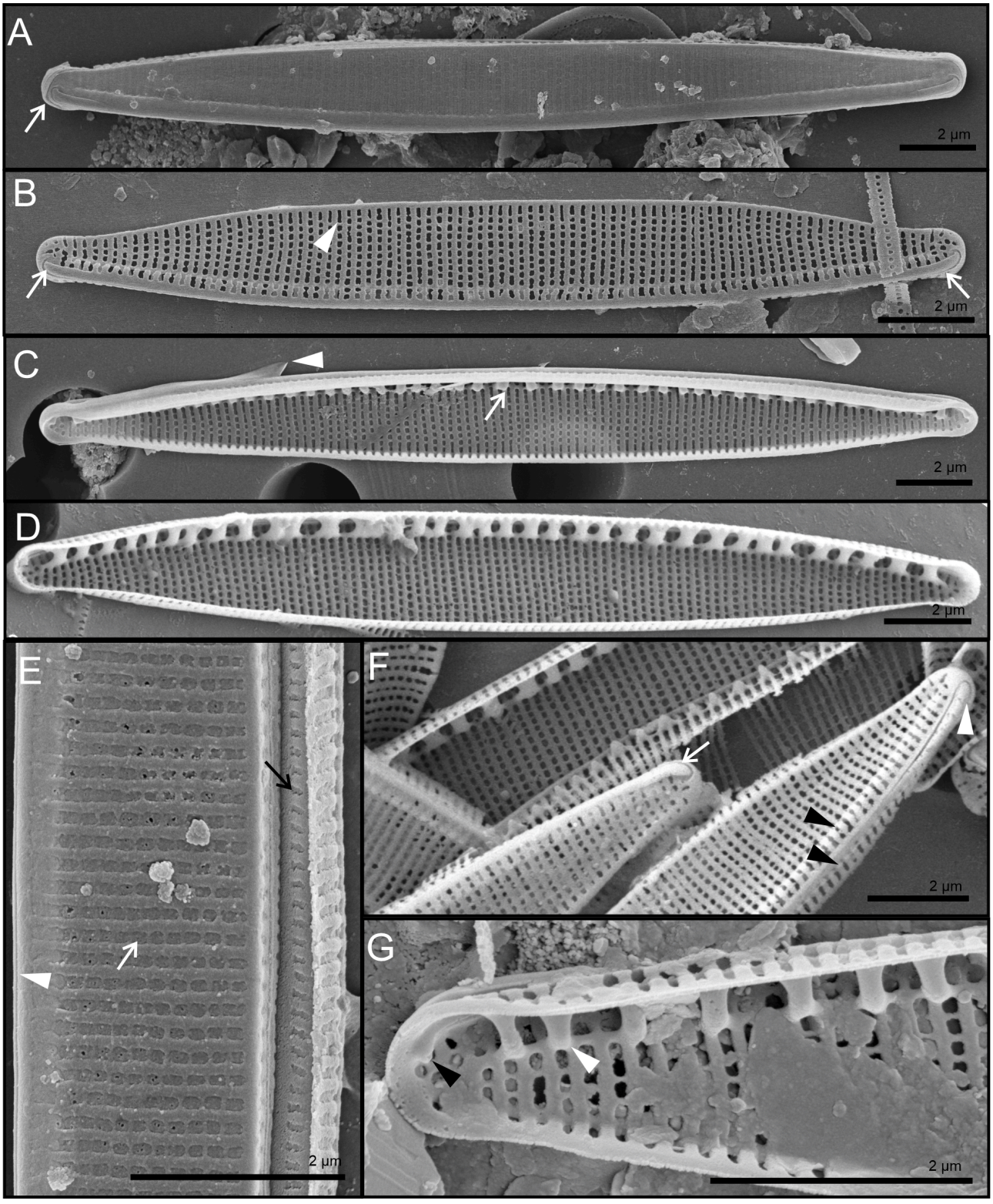



**Figure 5**

Scanning electron microscopy (SEM) micrographs of *Nitzschia eclipsis*sp. nov. from culture material. (**A–B**) External views of entire valves. (**A**) Valve with pore occlusions retained; arrow indicates the terminal

raphe fissure at the valve apex. (**B**) Valve with pore occlusions removed, revealing the uniseriate striae and poroid arrangement; arrows indicate the terminal raphe fissures, while arrowhead shows reduced vimines and fusion of adjacent areolae into elongate pores. (**C–D**) Internal views of entire valves showing short, narrow and regularly spaced fibulae, without a wider central interspace (arrow C). The obliquely tapered lateral end of a girdle band is visible alongside the valve (arrowhead C). (**E**) External detail of the valve showing the raphe canal wall and valvocopula; the black arrow indicates the single longitudinal row of well-developed poroids on the valvocopula, the white arrow indicates preserved pore occlusions, and the arrowhead marks the uninterrupted raphe slit lacking central raphe endings. (**F**) External views of valve apices showing poroid rows on the raphe canal wall (black arrowheads). The white arrow indicates a terminal raphe fissure strongly recurved towards the distal side of the valve and associated with an apical siliceous flap, whereas the white arrowhead indicates a terminal fissure recurved towards the proximal side, likewise associated with an apical siliceous flap. (**G**) Internal view of the valve apex showing a well-developed helictoglossa (black arrowhead), solid unornamented fibulae and virgae continuing towards the raphe canal (white arrowhead). Scale bars = 2 μm.

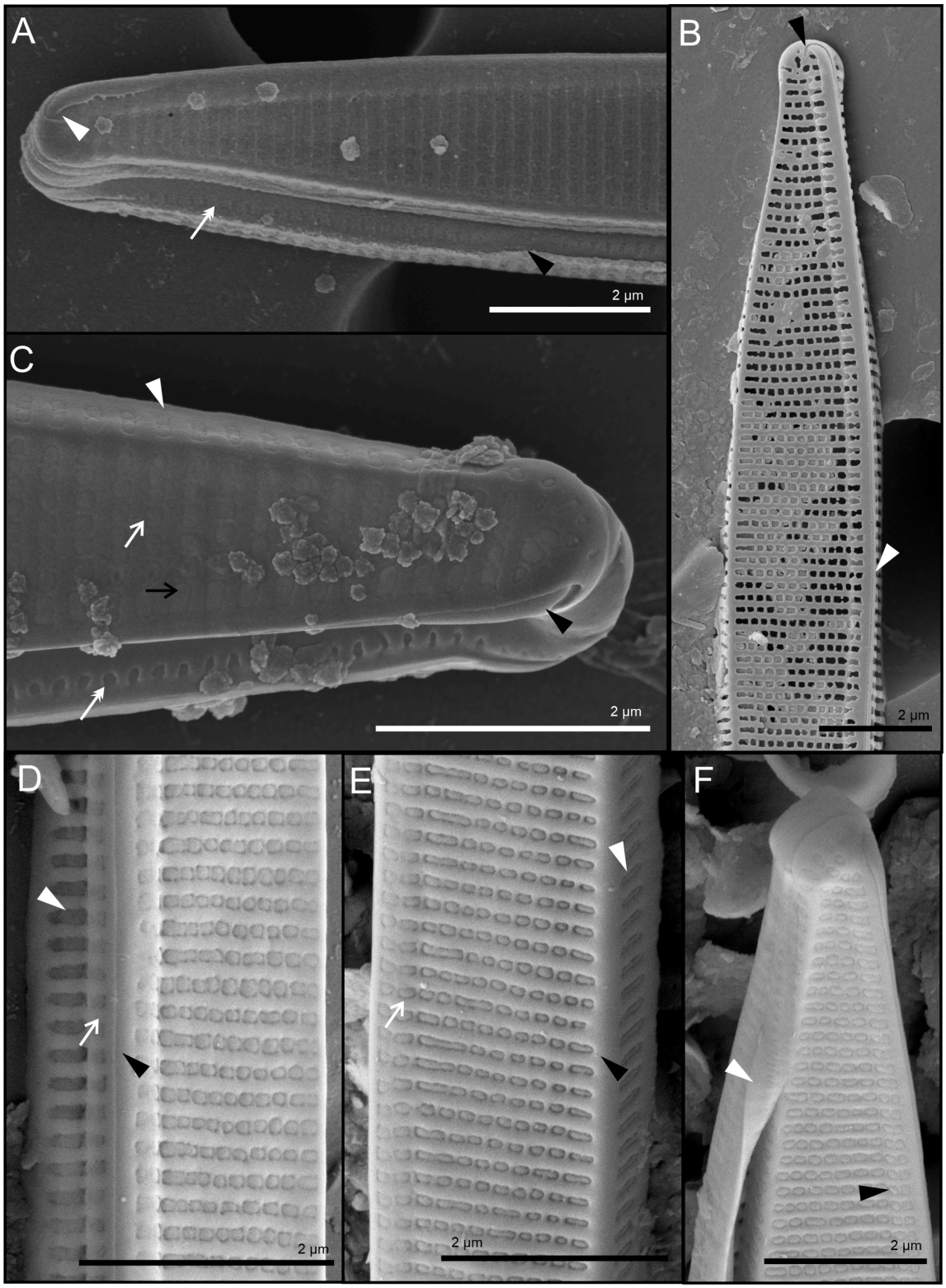



**Figure 6**

Scanning electron microscopy (SEM) micrographs of *Nitzschia eclipsis*sp. nov., external views of the valve apex and raphe canal. (**A**) Oblique view of a valve apex with pore occlusions retained; the white arrowhead indicates the terminal raphe fissure strongly recurved towards the distal side of the valve and associated with an apical siliceous flap, while the double arrow indicates the valvocopula bearing a single longitudinal row of well-developed poroids. Poroids on a girdle band become indistinct towards

one end of the valve; a junction between adjacent bands is not clearly resolved (black arrowhead). (**B**) Valve with pore occlusions removed. The white arrowhead marks the central part of the uninterrupted raphe slit, lacking central raphe endings. The black arrowhead indicates the terminal raphe fissure strongly recurved towards the distal side of the valve and associated with an apical siliceous flap. (**C**) Oblique view of the valve apex. The black arrow indicates a single longitudinal row of elongate pores on the raphe canal wall, whereas the white arrow indicates the typical poroids of the valve face. The white arrowhead marks longitudinal rows of poroids on the distal mantle, and the double-headed arrow indicates the valvocopula bearing a single row of well-developed poroids. The black arrowhead indicates the terminal raphe fissure recurved by nearly 180° towards the proximal side of the valve and associated with an apical siliceous flap. (**D**) The black arrowhead indicates the raphe. Pores are visible on both sides of the raphe on the raphe canal wall. At the distal raphe canal wall (arrow), the mantle-bearing elongate pores become visible (white arrowhead). (**E**) Detail of the distal mantle. The junction between the mantle (black arrowhead) and the valve is clearly visible. Mantle-bearing elongate pores (white arrowhead). The raphe canal wall bears two rows of pores (arrow). (**F**) Oblique view of the apex at approximately 35°. The white arrowhead indicates the reflexed valvocopula, apparently bearing a single row of pores. The black arrowhead indicates the double row of pores on the raphe canal wall. Scale bar = 2 µm.

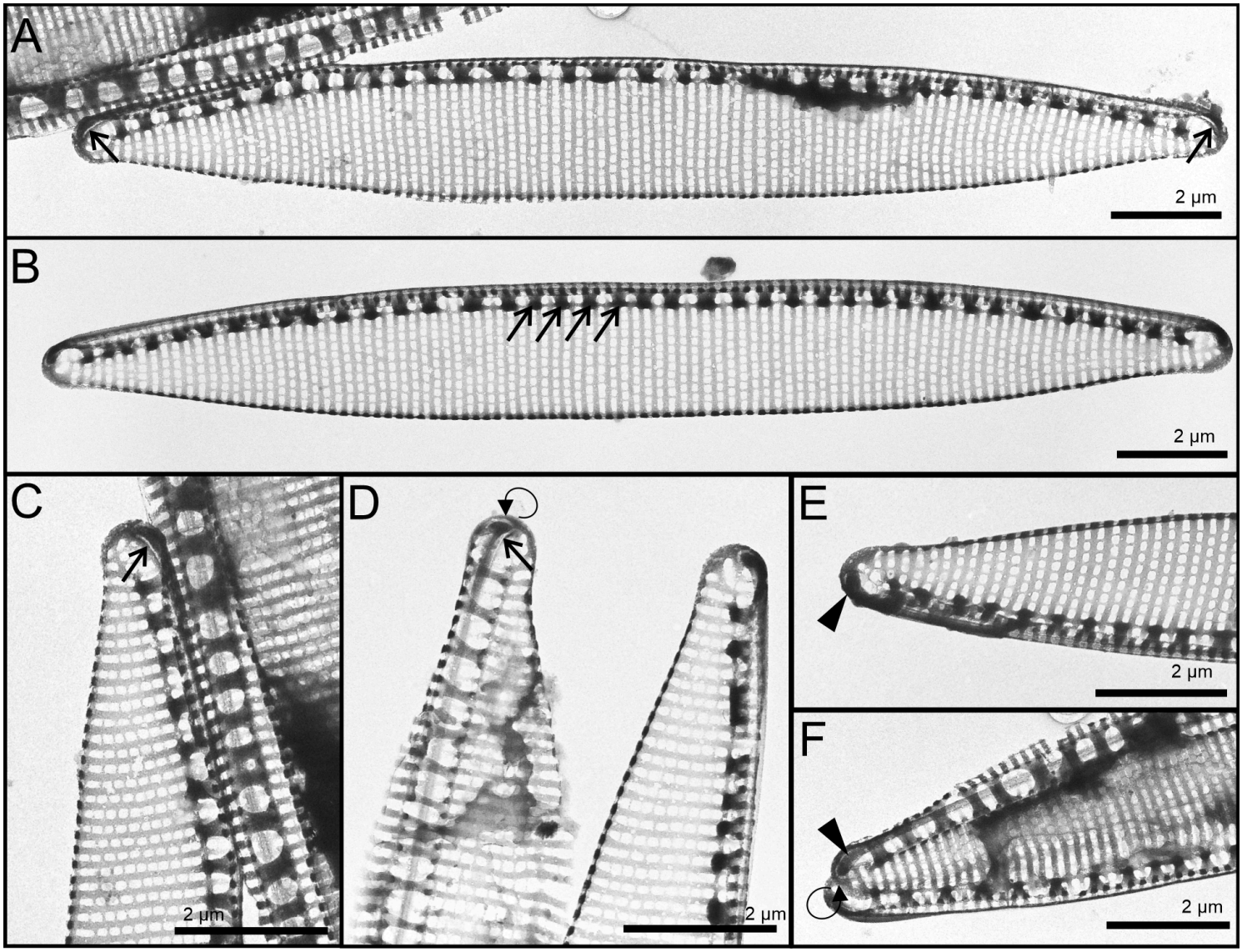
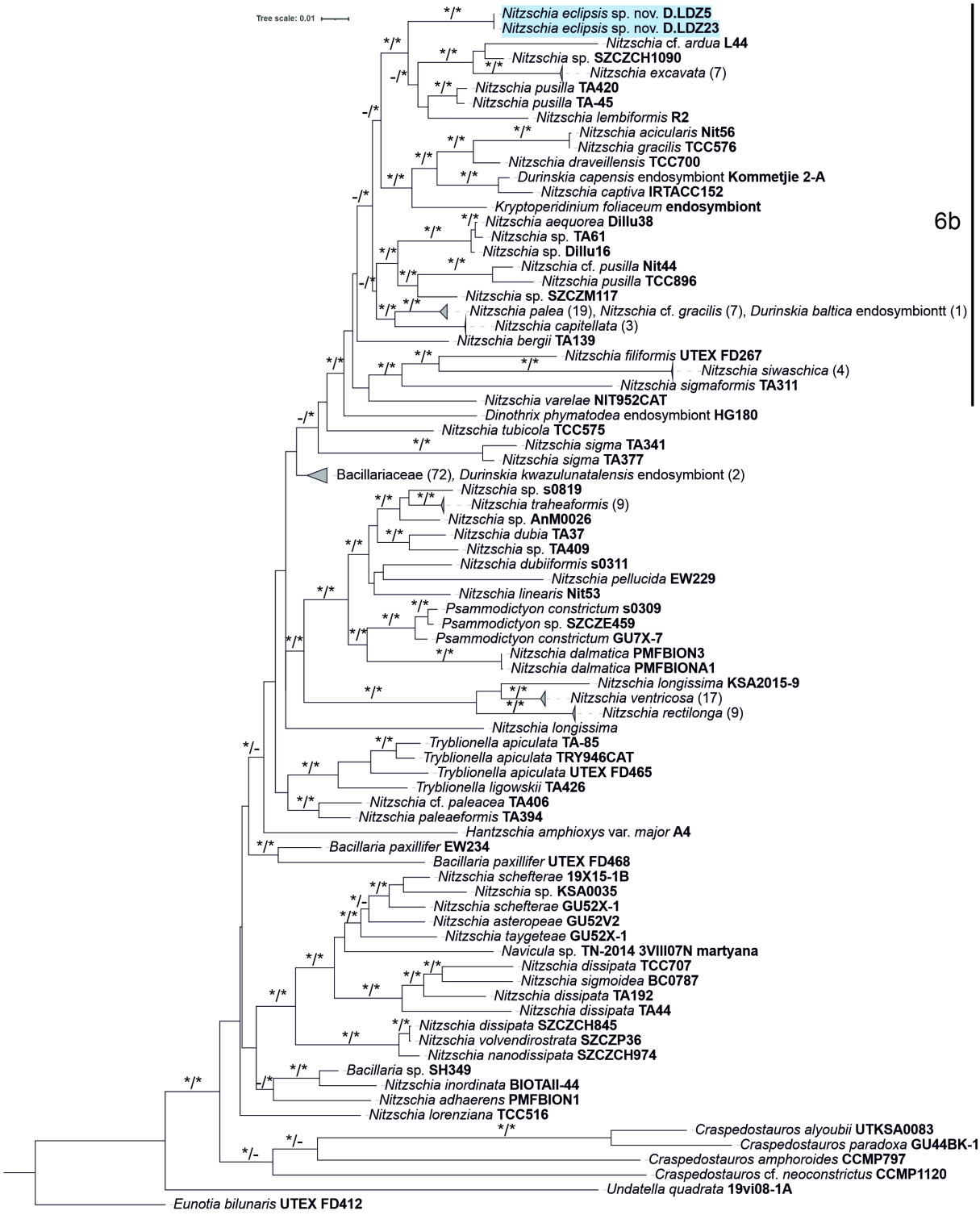



**Figure 7**

Transmission electron microscopy (TEM) micrographs of *Nitzschia eclipsis* sp. nov. (**A, B**) Entire valves. Arrows in A indicate the terminal raphe fissures visible at both apices; arrows in B indicate regularly spaced fibulae. (**C**) Enlarged view of one apex of the valve shown in A; the arrow indicates the terminal raphe fissure. (**D**) Apices of two valves. The straight arrow indicates the terminal raphe fissure, whereas the curved arrow indicates its recurvature through nearly 180°. (**E, F**) Details of valve apices. Arrowheads indicate the apical siliceous flap in each valve; the curved arrow in F indicates the terminal raphe fissure recurved through nearly 180°. Scale bars = 2 µm.




## Figure 8

Phylogenetic tree of the *Bacillariaceae*, with *Eunotia bilunaris* UTEX FD412 used as the outgroup, inferred from concatenated nuclear SSU rDNA and plastid *rbc*L and *psb*C sequences (total alignment length: 3,603 bp). The positions of the two strains of *Nitzschia eclipsis* sp. nov. are highlighted in blue. Branch support is presented in the order maximum likelihood/Bayesian inference (ML/BI). An asterisk indicates that the corresponding support value met the adopted threshold: UFBoot ≥95% for ML and PP ≥0.95 for

BI. Thus,*/*indicates that both thresholds were met, **/–* *indicates UFBoot ≥95% and PP <0.95, and –/** indicates UFBoot <95% and PP ≥0.95. Nodes with UFBoot values below 95% are not labelled. The topology shown was obtained from the ML analysis. Collapsed clades are represented by triangles, with numbers in parentheses indicating the number of terminal sequences included. Clade 6B is indicated following Mann et al. (2021). In the raw phylogenetic files provided as Supplementary Data S3 online, strains D.LDZ5 and D.LDZ23 are retained under the pre-description working label *Nitzschia* cf. *archibaldii*, which in this study refers to *Nitzschia eclipsis* sp. nov.

## Supplementary Files

This is a list of supplementary files associated with this preprint. Click to download.

- Supplementarycaptions.pdf
- SupplementaryTableS1.docx
- SupplementaryDataS2.xlsx
- SupplementaryDataS4.xlsx
- SupplementaryDataS3.zip
- SupplementaryFigureS5.tif
- SupplementaryFigureS6.pdf
- SupplementaryDataS7.fas
- SupplementaryTableS8.docx
- SupplementaryFigureS9.tif